



# Discovery of new 2-(3-(naphthalen-2-yl)-4,5-dihydro-1H-pyrazol-1-yl)thiazole derivatives with potential analgesic and anti-inflammatory activities: *In vitro*, *in vivo* and *in silico* investigations

Eman R. Mohammed<sup>a,\*</sup>, Aliaa H. Abd-El-Fatah<sup>a</sup>, Abdalla R. Mohamed<sup>b,\*</sup>, Marianne A. Mahrouse<sup>a</sup>, Mohammad A. Mohammad<sup>a</sup>

<sup>a</sup> Pharmaceutical Chemistry Department, Faculty of Pharmacy, Cairo University, Cairo 11562, Egypt

<sup>b</sup> Pharmaceutical Chemistry Department, Faculty of Pharmacy, Egyptian Russian University, Badr City, Cairo 11829, Egypt

## ARTICLE INFO

### Keywords:

COX-1/2  
Pyrazole clubbed thiazole  
Naphthalene  
Analgesic activity  
Anti-inflammatory agents  
Pharmacokinetic study

## ABSTRACT

Joining the global demand for the discovery of potent NSAIDs with minimized ulcerogenic effect, new pyrazole clubbed thiazole derivatives **5a-o** were designed and synthesized. The new derivatives were initially evaluated for their analgesic activity. Eight compounds **5a**, **5c**, **5d**, **5e**, **5f**, **5h**, **5m**, and **5o** showed higher activity than Indomethacin (potency = 105–130 % vs. 100 %). Subsequently, they were picked for further evaluation of their anti-inflammatory activity, ulcerogenic liability as well as toxicological studies. Derivatives **5h** and **5m** showed a potential % edema inhibition after 3 h (79.39 % and 72.12 %, respectively), with a promising safety profile and low ulcer indices (3.80 and 3.20, respectively). The two compounds **5h** and **5m** were subjected to *in vitro* COX-1 and COX-2 inhibition assay. The candidate **5h** showed nearly equipotent COX-1 inhibition ( $IC_{50}$  = 38.76 nM) compared to the non-selective reference drug Indomethacin ( $IC_{50}$  = 35.72 nM). Compound **5m** expressed significant inhibitory activities and a higher COX-2 selectivity index ( $IC_{50}$  = 87.74 nM, SI = 2.05) in comparison with Indomethacin (SI = 0.52), with less selectivity than Celecoxib (SI = 8.31). Simulation docking studies were carried out to gain insights into the binding interaction of compounds **5h** and **5m** in the vicinity of COX-1 and COX-2 enzymes that illustrated the importance of pyrazole clubbed thiazole core in hydrogen bonding interactions. The thiazole motif of compounds **5h** and **5m** exhibited a well orientation toward COX-1 Arg120 key residue by hydrogen bonding interactions. Compound **5h** revealed an additional arene-cation interaction with Arg120 that could rationalize its superior COX-1 inhibitory activity. Compounds **5h** and **5m** overlaid the co-crystallized ligand Celecoxib I differently in the active site of COX-2. Compound **5m** showed an enhanced accommodation with binding energy of – 6.13 vs. – 1.70 kcal/mol of compounds **5h**. The naphthalene ring of compound **5m** adopted the Celecoxib I benzene sulfonamide region that is stabilized by hydrogen-arene interactions with the hydrophobic sidechains of the key residues Ser339 and Phe504. Further, the core structure of compound **5m**, pyrazole clubbed thiazole, revealed deeper hydrophobic interactions with Ala513, Leu517 and Val509 residues. Finally, a sensitive and accurate UPLC-MS/MS method was developed for the simultaneous estimation of some selected promising pyrazole derivatives in rat plasma. Accordingly, compounds **5h** and **5m** were suggested to be promising potent analgesic and anti-inflammatory agents with improved safety profiles and a novel COX isozyme modulation activity.

## 1. Introduction

Pain and inflammation are augmented with a wide range of diseases and medical conditions. The inflammation process is regarded to the immune system defense response toward the abnormal physiological events [1–3]. The inflammatory related events involve characteristic

features such as edema, swelling, pain, fever, and loss of tissue function, which on the molecular level, they exacerbate a network of signaling pathways such as NF- $\kappa$ B, MAPK, and JAK-STAT [3]. Unfortunately, the persistence of inflammation for long duration without medical intervention could lead to cancer [4]. The signaling molecules are controlled by pro-inflammatory biomarkers and cytokines that are accompanied by

\* Corresponding authors.

E-mail addresses: [eman.raafat@pharma.cu.edu.eg](mailto:eman.raafat@pharma.cu.edu.eg) (E.R. Mohammed), [abdallaharafa@eru.edu.eg](mailto:abdallaharafa@eru.edu.eg) (A.R. Mohamed).

<https://doi.org/10.1016/j.bioorg.2024.107372>

Received 15 March 2024; Received in revised form 5 April 2024; Accepted 12 April 2024

Available online 17 April 2024

0045-2068/© 2024 Elsevier Inc. All rights reserved.

morbidity and/or mortality in several disease such as cardiovascular [1], lung [5], hepatitis [6], Alzheimer's [7], Parkinson's [8], and cancer diseases [4,9], in addition to arthritis [10]. The severity and complexation of inflammatory diseases, ranging from acute to chronic associated cases, render the search for new anti-inflammatory agents a crucial importance.

Non-steroidal anti-inflammatory drugs (NSAIDs) inhibit cyclooxygenase enzymes (COX-1 and COX-2) that catalyze the conversion of arachidonic acid to prostaglandins (PGs), prostacyclin (PGI<sub>2</sub>), and thromboxane A<sub>2</sub> (TXA<sub>2</sub>) [11]. Thus, the membrane associated proteins COX enzymes have an important role in the induction of homeostatic functions and pro-inflammatory PGs. Although the later process is mainly controlled by COX-2 isoform, a number of studies have suggested the implication of COX-1 in the early stages of inflammation that mediate prostanoid synthesis and during the progression of inflammation [12]. However, the selective targeting of COX-2 enzyme provided promising anti-inflammatory activity, with reduced gastrointestinal ulceration, nephrotoxicity, platelet defect and bleeding side effects that are commonly accounted to the inhibition of COX-1 isozyme [13]. COX-1 and COX-2 have a high degree of amino-acid sequence similarity (67 %), structural topology, and the same catalytic mechanism [14,15]. However, COX-2 isozyme permits a larger ligand to access for binding relaying on one of the major residue differences that discriminate it from COX-1; Val523 vs. Ile523, respectively [16].

Pyrazole ring is a privilege heterocyclic scaffold that has been incorporated in several active lead compounds. Several pyrazole containing derivatives had received FDA approval for their contribution in multiple medical conditions treatment [17–19]. Celecoxib I (Fig. 1) was introduced as a selective COX-2 inhibitor, retaining an important structural feature for this activity, viz central pyrazole ring that has two adjacent phenyl rings, and one of them is substituted with 4-aminosulfonyl group [20]. Several attempts studied these features to produce more amenable analogs by retaining the two adjacent phenyl rings with either aminosulfonyl or methanesulfonyl moiety, changing the central

ring to furanone or isoxazol such as Rofecoxib II and Valdecoxib III (Fig. 1), respectively [20–23]. Meanwhile, great concerns have been accounted for these Coxib derivatives for their cardiovascular adverse effect [24,25]. The major effort to explore the Celecoxib I pharmacophoric features was directed toward utilizing different pattern of substitutions on the pyrazole heterocyclic ring, retaining the aminosulfonylphenyl substitution [22,26,27].

Meanwhile, the thiazole motif is present in the architecture of clinically approved anti-inflammatory and analgesic drugs such as Meloxicam IV [28], which is a selective inhibitor of COX-2, for management of osteoarthritis and other inflammatory related disorders, in addition to the NSAID Fentiazac V (Fig. 1) [29]. The thiazole based derivative Darbufelone VI showed promising anti-inflammatory and analgesic activity by exerting a preferential COX-2 inhibition [30]. The direct attachment of thiazole motif to pyrazole heterocyclic ring introduced a great contribution in various pharmacological activities that include the potential alleviation of inflammatory diseases [31–34]. Modifications that produced a thiazole-celecoxib analogues has provided promising results regarding the COX-2 selective inhibition, using 4,5-dihydro-1H-pyrazole scaffold [23].

At the same time, naturally and synthetic naphthalene derivatives showed broad spectrum of pharmacological activities that renders naphthalene, as an aromatic conjugated system, a privilege bicyclic system in drug discovery. The naphthalene-based derivatives Naproxen VII and Nabumetone VIII (Fig. 1) are FDA approved anti-inflammatory drugs that are used in several inflammatory diseases. The later one is a prodrug, and its active form (compound IX, Fig. 1) is preferentially an inhibitor of COX-2 [10]. Subsequently, several reports addressed the enhancement in anti-inflammatory activity by varying heterocyclic substitutions at the  $\beta$ -carbon of naphthalene ring [35,36].

The present study aims to introduce novel pyrazole-based anti-inflammatory and analgesic candidates by exploring further anti-inflammatory pharmacophoric criterions. The rational design relayed on a multifactorial hybridization approach that is devoid from

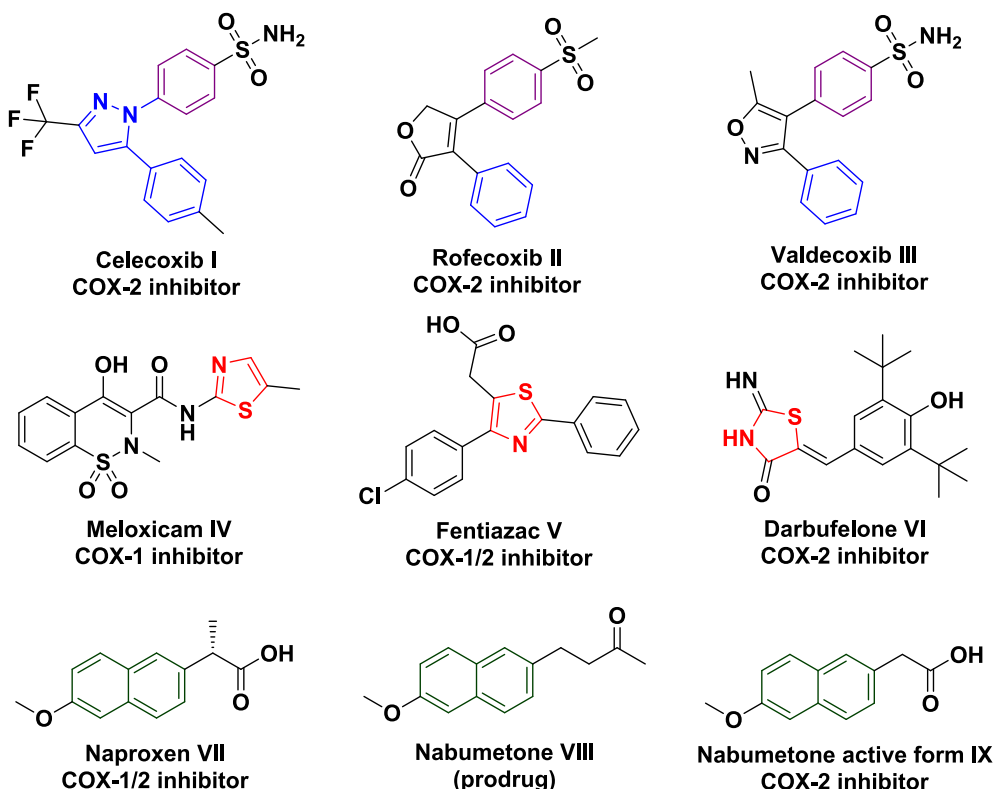


Fig. 1. Chemical structure of clinically approved anti-inflammatory drugs.

carboxylic acid and benzene sulfonamide functions that are commonly indispensable for the traditional NSAID and Coxibs, respectively, which could enhance the new series safety profile. As shown in Fig. 2, a molecular hybridization was performed by clubbing thiazole, which is the parent scaffold in compounds V and VI, to the central pyrazole ring N-1 of Celecoxib I. The molecular framework retained the two phenyls of Celecoxib I, wherein one of them appended the thiazole ring at C-4 that mimics the pharmacophoric feature of Fentiazac V. The other one was kept at the pyrazole C-3, as Celecoxib I, to afford the pyrazole clubbed thiazole X.

Noteworthy, the introduction of a bulky aromatic conjugated substitution at pyrazole C-5 gives a surpassed selective activity against COX-2, with less gastric ulceration effect compared to Celecoxib I [37]. Thus, the novel Coxib pharmacophoric pattern X was further hybridized with naphthalene motif at C-5 of pyrazole ring. A study of structure activity relationship of the produced molecular arrangement was achieved by varying substations at the two phenyl rings to provide the targeted compounds 5a-o. The new pyrazole derivatives were evaluated for their *in vivo* analgesic activity. Additionally, the anti-inflammatory and gastric ulcerogenic effects were evaluated for the promising analgesic derivatives. The most promising compounds were screened for their COX-1 and COX-2 inhibitory activity to study the utilized approach effect on the selectivity indices. Furthermore, molecular docking study was performed to gain insights about the possible binding modes within the active site of COX enzymes.

## 2. Results and discussion

### 2.1. Chemistry

The synthetic pathway adopted to furnish the target pyrazole derivatives 5a-o was illustrated in Scheme 1. The known intermediates 2a-e [38–42], 3a-d [43,44] and 4a-c [45–47] were synthesized according to the reported procedures. Cyclization reaction that afforded the final pyrazole derivatives 5a-o was achieved by reacting the pyrazole-1-carbothioamide intermediates 3a-e with the appropriate phenacyl bromide derivative 4a-c in absolute ethanol.

Compounds 5a-o were confirmed using their spectral and analytical data.  $^1\text{H}$  NMR spectra of derivatives 5a-o revealed three characteristic doublet of doublet signals corresponding to the pyrazoline ring three protons of saturation ( $\text{CH}_2$  and  $\text{CH}$ ) at 3.42–3.50, 3.97–4.16 and 5.63–5.78 ppm. Additionally, their  $^{13}\text{C}$  NMR spectra indicated the appearance of two signals in aliphatic range representing  $\text{CH}_2$  and  $\text{CH}$  carbons of pyrazoline moiety at 43.07–43.87 and 64.10–64.89 ppm, respectively. Moreover,  $^1\text{H}$  NMR spectra of compounds 5d, 5f, 5g, 5h, 5i, 5j, and 5n demonstrated the appearance of singlet signals assigned to  $\text{OCH}_3$  protons at 3.72–3.81 ppm.  $^{13}\text{C}$  NMR spectra of the same compounds revealed the appearance of new signal attributed to  $\text{OCH}_3$  carbons at 55.28–55.57 ppm.  $^1\text{H}$  NMR spectra of compounds 5e, 5j, and 5o displayed singlet signal assigned to  $\text{N}(\text{CH}_3)_2$  protons at 2.84–2.93 ppm. Moreover, signals of  $\text{N}(\text{CH}_3)_2$  carbons of compounds 5e, 5j, and 5o

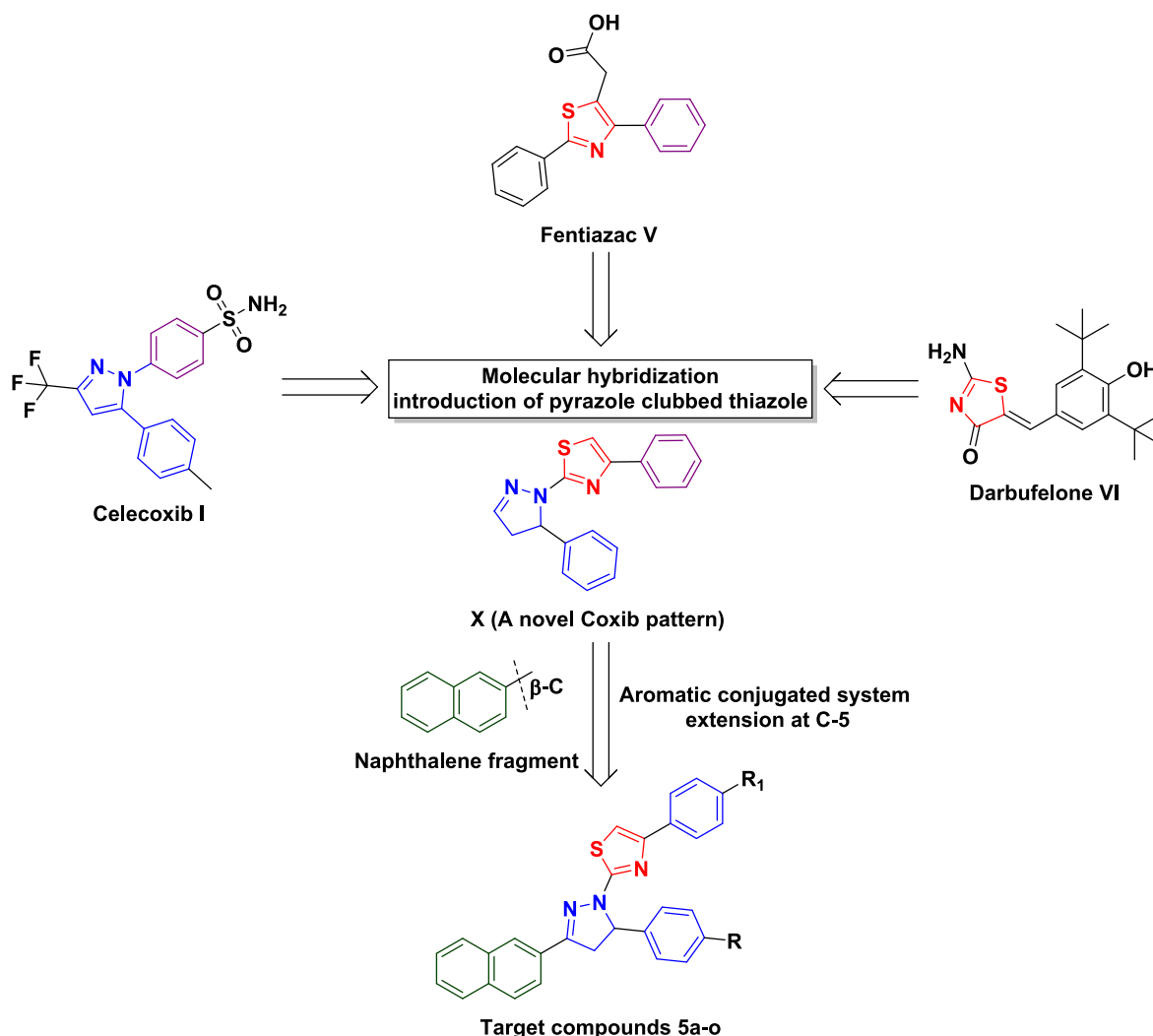
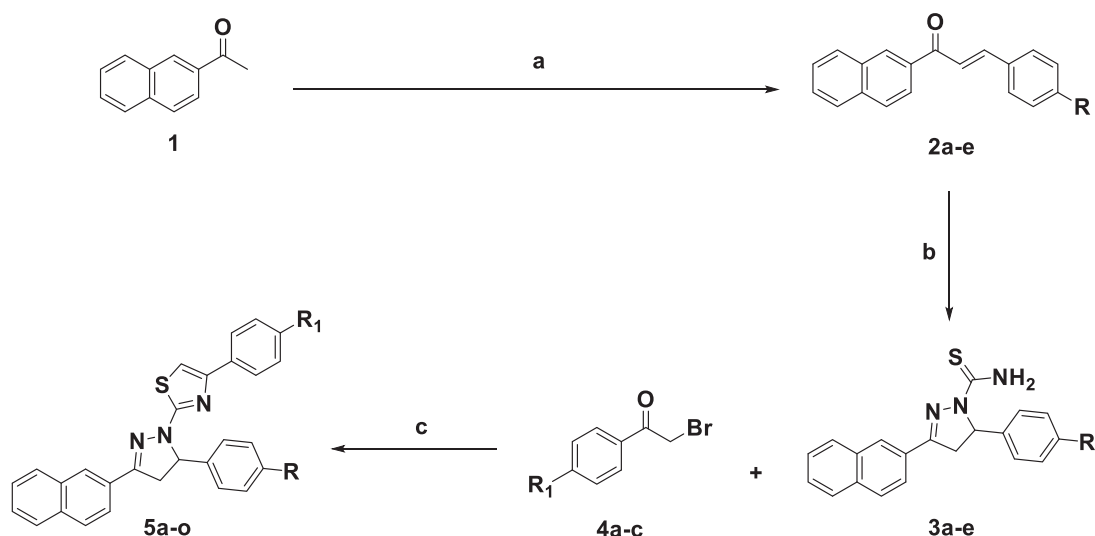


Fig. 2. Diagrammatic representation for the rational design of the new targeted anti-inflammatory candidates.



Compound	R	R <sub>1</sub>
<b>5a</b>	H	Cl
<b>5b</b>	Cl	Cl
<b>5c</b>	F	Cl
<b>5d</b>	OCH <sub>3</sub>	Cl
<b>5e</b>	N(CH <sub>3</sub> ) <sub>2</sub>	Cl
<b>5f</b>	H	OCH <sub>3</sub>
<b>5g</b>	Cl	OCH <sub>3</sub>
<b>5h</b>	F	OCH <sub>3</sub>
<b>5i</b>	OCH <sub>3</sub>	OCH <sub>3</sub>
<b>5j</b>	N(CH <sub>3</sub> ) <sub>2</sub>	OCH <sub>3</sub>
<b>5k</b>	H	F
<b>5l</b>	Cl	F
<b>5m</b>	F	F
<b>5n</b>	OCH <sub>3</sub>	F
<b>5o</b>	N(CH <sub>3</sub> ) <sub>2</sub>	F

Compound	R <sub>1</sub>
<b>4a</b>	Cl
<b>4b</b>	OCH <sub>3</sub>
<b>4c</b>	F

Compound	R
<b>2a, 3a</b>	H
<b>2b, 3b</b>	Cl
<b>2c, 3c</b>	F
<b>2d, 3d</b>	OCH <sub>3</sub>
<b>2e, 3e</b>	N(CH <sub>3</sub> ) <sub>2</sub>

**Scheme.1.** Reagents and reaction conditions: a) 4-Un/substituted benzaldehyde, 10 % aqueous sodium hydroxide solution, ethanol, stirring overnight, b) Thiosemicarbazide, sodium hydroxide pellets, ethanol, reflux, 8 h, c) Ethanol, reflux, 2–6 h.

appeared in <sup>13</sup>C NMR spectra at 40.52–40.54 ppm.

## 2.2. Biological evaluation

### 2.2.1. Analgesic activity evaluation

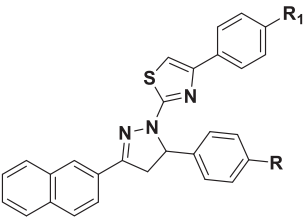
The newly synthesized pyrazole-based derivatives **5a-o** were evaluated for their analgesic activity. The *p*-benzoquinone-induced writhing method in mice was utilized using Indomethacin as a reference standard, according to Okun *et. al.* [48]. The adopted pharmacophoric

hybridization strategy resulted in a remarkable analgesic activity of all the newly synthesized compounds **5a-o** with potency at the range of 80–130 %, compared to indomethacin (potency = 100 %).

As illustrated in Table 1, compounds **5a**, **5c**, **5d**, **5e**, **5f**, **5h**, **5m**, and **5o** showed higher activity than Indomethacin (potency = 105–130 % vs. 100 %). These compounds bear different substitutions at the two phenyl rings. However, the close investigation of structure activity relationship revealed the mutual effect of substitutions. The combination of electron withdrawing group at the phenyl sidechain of thiazole motif (chloro or

**Table 1**

Analgesic activity of compounds **5a-o** and indomethacin [number of mice (n) = 5, at dose 28 µm/Kg].



Compound	R	R <sub>1</sub>	Writhing reflex ± SEM	% Protection	% Potency **
<b>5a</b>	H	Cl	1.4 ± 0.24 *	87.04	117.51
<b>5b</b>	Cl	Cl	2.8 ± 2.06 *	74.07	100
<b>5c</b>	F	Cl	2.4 ± 1.08 *	77.78	105
<b>5d</b>	OCH <sub>3</sub>	Cl	1.2 ± 0.73 *	88.89	120
<b>5e</b>	N(CH <sub>3</sub> ) <sub>2</sub>	Cl	1.4 ± 0.24 *	87.04	117.51
<b>5f</b>	H	OCH <sub>3</sub>	1 ± 0 *	90.74	122.51
<b>5g</b>	Cl	OCH <sub>3</sub>	2.8 ± 0.49 *	74.07	100
<b>5h</b>	F	OCH <sub>3</sub>	2 ± 1.10 *	81.48	110
<b>5i</b>	OCH <sub>3</sub>	OCH <sub>3</sub>	4.4 ± 0.24 *	59.26	80
<b>5j</b>	N(CH <sub>3</sub> ) <sub>2</sub>	OCH <sub>3</sub>	4 ± 0.84 *	62.96	85
<b>5k</b>	H	F	3.4 ± 1.4 *	68.52	92.51
<b>5l</b>	Cl	F	2.8 ± 0.92 *	74.07	100
<b>5m</b>	F	F	1.8 ± 0.92 *	83.33	112.50
<b>5n</b>	OCH <sub>3</sub>	F	2.8 ± 1.20 *	74.07	100
<b>5o</b>	N(CH <sub>3</sub> ) <sub>2</sub>	F	0.4 ± 0.24 *	96.03	130
<b>Control</b>	—	—	10.8 ± 1.36	0	0
<b>Indomethacin</b>	—	—	2.8 ± 2.06 *	74.07	100

Statistical analysis was carried out by one-way ANOVA test.

\* Significance difference from the control value at p < 0.05.

\*\* % Potency = % Protection relative to Indomethacin

fluoro) and electron donating group (methoxy or dimethylamine) at the other phenyl sidechain attached to the pyrazole scaffold retained a potent analgesic activity, such as compounds **5d** (potency = 120 %) and **5o** (potency = 130 %), respectively. Interestingly, the potency was slightly decreased by inverting the pattern of substitution between the two phenyls such as compounds **5g** (potency = 100 %) and **5h** (potency = 110 %) that retain 4-(4-methoxyphenyl)thiazole sidechain along with chloro or fluoro groups, respectively, at the other phenyl sidechain.

Noteworthy, compound **5f** 4-(4-methoxyphenyl)thiazole sidechain restored a higher activity than most compounds (potency = 122.51 %) by using the unsubstituted 4-(phenyl)thiazole, which highlights a kind of exchangeable rules between both fragment for optimum activity. Meanwhile, using two electron donating groups at the two phenyl sidechains dropped the activity in compounds **5i** and **5j** that showed lower potency (80 and 85, respectively) than Indomethacin. The halogen substitutions (electron withdrawing groups) at the 4-(phenyl)thiazole and 5-(phenyl)-pyrazole sides revealed a compromised activity with preferential potency for the dual using of a smaller fluoro group; compound **5m** (potency = 112.5 %).

### 2.2.2. Anti-inflammatory screening

Compounds **5a**, **5c**, **5d**, **5e**, **5f**, **5h**, **5m**, and **5o** showed the highest analgesic activity among all the newly synthesized pyrazole derivatives. Subsequently, they were picked for further screening of their anti-inflammatory potential by the use of carrageenan-induced rat paw edema model, according to previously reported method [49]. The selected compounds along with Indomethacin, as a reference drug, were evaluated for the inhibition of induced edema. The % potency were calculated relative to Indomethacin (potency = 100 %) at two different time intervals (2 h and 3 h) and were recorded in Table 2.

**Table 2**

Anti-inflammatory effect of compounds **5a**, **5c**, **5d**, **5e**, **5f**, **5h**, **5m**, and **5o**, in addition to Indomethacin, on carrageenan induced edema of the hind paw in rats [number of rats (n) = 5, at dose of 28 µm/Kg].

Cpd. No.	Edema (mm) ± SEM (Inhibition of inflammation %)		Potency % 2h 3h
	2h	3h	
<b>5a</b>	0.86 ± 0.08* (46.25)	0.62 ± 0.04* (62.42)	62.71 93.63
<b>5c</b>	0.53 ± 0.12* (66.87)	0.43 ± 0.13* (73.94)	90.67 110.90
<b>5d</b>	0.77 ± 0.07* (51.88)	0.41 ± 0.04* (75.15)	70.35 112.72
<b>5e</b>	0.94 ± 0.02* (41.25)	0.72 ± 0.01* (56.36)	55.93 84.54
<b>5f</b>	0.68 ± 0.08* (57.50)	0.46 ± 0.04* (72.12)	77.97 108.17
<b>5h</b>	0.60 ± 0.05* (62.50)	0.34 ± 0.04* (79.39)	84.75 119.08
<b>5m</b>	0.71 ± 0.06* (55.62)	0.46 ± 0.04* (72.12)	75.42 108.17
<b>5o</b>	0.87 ± 0.05* (45.63)	0.72 ± 0.01* (56.36)	61.87 84.54
<b>Control</b>	1.60 ± 0.11	1.65 ± 0.13	0 0
<b>Indomethacin</b>	0.42 ± 0.18* (73.75)	0.55 ± 0.20 (66.67)	100 100

Statistical analysis was carried out by one-way ANOVA test.

\* Significance difference from the control value at p < 0.001.

It was found that all the tested compounds displayed good anti-inflammatory activity. After 2 h, all the eight tested compounds **5a**, **5c**, **5d**, **5e**, **5f**, **5h**, **5m**, and **5o** exhibited moderate activity ranging from 41.25 % to 66.87 % inflammatory inhibition compared to indomethacin (73.75 % inhibition). The anti-inflammatory activity of all tested compounds revealed enhancement after 3 h (edema inhibition = 56.36–79.39 %), compared to the reference standard (edema inhibition = 66.67 %). Meanwhile, compounds **5c**, **5d**, **5f**, **5h**, and **5m** exhibited a promising anti-inflammatory activity (edema inhibition = 72.12–79.39 %) that surpassed the reference standard Indomethacin.

### 2.2.3. Ulcerogenic liability

Derivatives **5a**, **5c**, **5d**, **5e**, **5f**, **5h**, **5m**, and **5o** that exhibited a promising analgesic activity were further investigated for their ulcerogenic potential using Indomethacin as a reference standard, according to reported method by Meshali *et al* [50]. As illustrated in Table 3, the tested compounds revealed a remarkable gastrointestinal track (GIT) tolerance than Indomethacin. It is worthily mentioned that compounds **5e**, **5h**, and **5m** displayed the lowest ulcerogenic effect, as indicated by their ulcer indices 0, 3.8, and 3.20, respectively (Supplementary Materials, Fig. 1S).

### 2.2.4. Toxicological study

Toxicological study of the most potent analgesic compounds **5a**, **5c**,

**Table 3**

Ulcerogenic effect Compounds **5a**, **5c**, **5d**, **5e**, **5f**, **5h**, **5m**, and **5o**, in addition to Indomethacin and in rats [number of rats (n) = 5, at dose of 28 µm/Kg].

Cpd. No.	% Incidence divided by 10	Average no. of ulcer	Average severity	Ulcer index
<b>Control</b>	0	0	0	0
<b>indomethacin</b>	10	4.6	1.56	16.16
<b>5a</b>	10	3.8	1.15	14.95
<b>5c</b>	6	1.80	1.33	9.13
<b>5d</b>	6	1	1.20	8.20
<b>5e</b>	0	0	0	0
<b>5f</b>	10	3	1.40	14.40
<b>5h</b>	2	0.8	1	3.8
<b>5m</b>	2	0.2	1	3.20
<b>5o</b>	2	0.8	1.25	4.05



**5d**, **5e**, **5f**, **5h**, **5m**, and **5o** was carried out using Finney's method [51]. All the examined compounds demonstrated a high safety margin. After 24 h of observation, no animal was killed by intraperitoneal injection of dosages up to 10 times of the used analgesic dose, with the exception of compound **5m**, which was safe at doses up to 5 times.

### 2.2.5. COX-1/2 inhibitory activity evaluation

Compounds **5h** and **5m** were selected for *in vitro* screening of COX-1 and COX-2 inhibitory activity. By examining the whole obtained biological results, both compounds maintained collectively good analgesic and anti-inflammatory activities with minimized ulcerogenic effect. Derivatives **5h** and **5m** showed a high analgesic activity with % potency of 110 and 112.50 %, respectively, and a potential % edema inhibition after 3 h (79.39 % and 72.12 %, respectively), with a promising safety profile and low ulcer indices (3.80 and 3.20, respectively). Thus, compounds **5h** and **5m** were evaluated for *in vitro* COX-1 and COX-2 inhibition, according to reported methodology [52]. As examples of selective COX-2 and non-selective inhibitors, Celecoxib I and Indomethacin were used as reference drugs, respectively.

As shown in Table 4, compounds **5h** and **5m** showed a promising anti-COX activity. Compound **5h** that retains the 4-(4-methoxyphenyl) thiazole sidechain showed nearly equipotent COX-1 inhibition ( $IC_{50}$  = 38.76 nM) compared to the non-selective reference drug Indomethacin ( $IC_{50}$  = 35.72 nM). Additionally, it revealed less COX-2 inhibition ( $IC_{50}$  = 166.50 nM) than Celecoxib I and indomethacin ( $IC_{50}$  = 53.30 and 68.74 nM, respectively). Meanwhile, compound **5m** that has two fluoro groups at the two phenyl sidechains showed a higher COX-2 selectivity index ( $IC_{50}$  = 87.74 nM, SI = 2.05) than Indomethacin (SI = 0.52), while it was less selective than Celecoxib I (SI = 8.31). The *in vitro* findings revealed that both compounds are interesting COX modulators, and specifically they were found to be correlating recently described phenylthiazole derivatives [53,54].

### 2.3. Molecular modeling studies

The protein structure of COX enzyme exhibits a hydrophobic channel between the membrane-binding region and the haem that ends by the active site. Therefore, the natural substrate (arachidonic acid) revealed excessive van der Waals contacts with the crystal structure hydrophobic regions [15]. Compounds **5h,m** revealed superior *in vivo* analgesic and anti-inflammatory activities, in addition to a potent *in vitro* COX-1 and COX-2 inhibitory activity. To gain more insights into compounds **5h,m** possible binding interactions in the active sites of COX-1 and COX-2 isoforms, molecular docking studies were performed using Molecular Operating Environment (MOE 2019.0101) software package. Compounds **5h,m** were docked into the active site of COX-1 enzyme co-crystallized with Ibuprofen (PDB: 1EQG) [55], and COX-2 enzyme co-crystallized with Celecoxib I (PDB: 3LN1) [56]. Validation of docking protocols were achieved by docking of Ibuprofen and Celecoxib I, the co-crystallized ligands, which regenerated the binding pattern in COX-1 and COX-2 active sites, with energy scores of - 7.48 and - 9.92 kcal/mol and RMSD values of 0.8765 and 0.0553 Å, respectively. The docking

**Table 4**

Inhibitory activity of compounds **5m** and **5h**, along with the reference standards Celecoxib I and indomethacin against COX-1 and COX-2 enzymes.

Compound	$IC_{50}$ (nM) <sup>a</sup>		SI <sup>b</sup> (COX-1/COX-2)
	COX-1	COX-2	
<b>5h</b>	38.76 ± 3.88	166.5 ± 7.97	0.23
<b>5m</b>	179.70 ± 4.57	87.74 ± 5.22	2.05
Celecoxib I	442.70 ± 4.45	53.30 ± 5.15	8.31
Indomethacin	35.72 ± 5.82	68.74 ± 4.79	0.52

<sup>a</sup> Data are presented as  $IC_{50}$  values (Mean ± SD) of three independent experiments.

<sup>b</sup> The *in vitro* COX-2 selectivity index (COX-1/COX-2).

poses showed that all the key interactions were reproduced by the co-crystallized ligands with the binding site hot spots in the active site of COX-1 (Tyr355, Arg120) and COX-2 (Leu338, Ser339), Supplementary Material (Figures 10S and 11S).

Regarding COX-1 active site, compounds **5h,m** showed a well accommodation with binding energy of - 5.95 and - 5.06 kcal/mol (Fig. 3A-D). The 4-methoxyphenyl and 4-fluorophenyl sidechains of thiazole motif of compounds **5h** and **5m**, respectively, overlaid the ligand Ibuprofen site. Compound **5h** 4-methoxyphenyl sidechain maintained hydrophobic interactions with Ile523, Leu352, Trp387, Ala527 and Phe518 residues, while compound **5m** 4-fluorophenyl maintained the same interactions with Val119, Ala527, Leu352, Leu53, Leu359 and Ile89 residues, lining the active site cavity. The thiazole ring points toward Arg120 key residue, which forms hydrogen bonding with the thiazole N-3 of both compounds. Additionally, compound **5h** revealed arene-cation interaction with Arg120. Naphthalene ring of each compound extended between Ile89 and Leu115 residues, which was stabilized by hydrophobic interactions. Noteworthy, compound **5h** revealed a better recognition than **5m** in the active site, which rationalizes the *in vitro* activity against COX-1 enzyme ( $IC_{50}$  = 38.76 and 179.70 nM, respectively).

Concerning the molecular docking of compounds **5h,m** in the active site of COX-2, they overlaid the co-crystallized ligand differently with binding energy of - 1.70 and - 6.13 kcal/mol, respectively (Fig. 4A-D). Compound **5h** revealed a reasonable extension of the 4-(4-methoxyphenyl)thiazole fragment toward Ser339 residue, forming two unusual hydrogen bonding interactions with HSD75 and Gln178 residues. The pyrazole clubbed thiazole core exhibited two hydrogen bonding with Ala513 and Arg106 residues (N-2 of pyrazole and S-1 of thiazole, respectively) in the vicinity of active site. While, the naphthalene sidechain extended to the top of the active site, sweeping out approximately the same hydrophobic interaction of the 4-tolyl ring of Celecoxib I with the hydrophobic sidechain of Val509 and Leu345. The directly attached 4-phenyl ring at C-5 of pyrazole scaffold oriented as the trifluoromethyl group of Celecoxib I that formed van der Waals interactions with Met99 and Val335 residues.

Meanwhile, the naphthalene ring of compound **5m** adopted the Celecoxib I benzene sulfonamide region, which was sandwiched by hydrogen-arene interactions with the hydrophobic sidechains of the key residues Ser339 and Phe504. Moreover, the pyrazole clubbed thiazole core of compound **5m** revealed three hydrogen bonding interactions with the active site vicinity amino-acids Val509 (N-2 of pyrazole ring), Ser516 and Leu517 (S-1 and N-3 of thiazole ring, respectively). The core structure of compound **5m**, pyrazole clubbed thiazole, revealed hydrophobic interactions with Ala513, Leu517 and Val509. Hydrophobic interactions maintained the two 4-fluorophenyl sidechains to fill two different hydrophobic pockets. One of them is lined by Leu103, Met99, Leu370 and Val102 residues. The former residue showed a distant hydrogen bonding interaction with the fluoro group of 4-(4-fluorophenyl)-thiazole fragment. The other hydrophobic region is lined by Val335, Trp373 and Phe367. Thus, the current modeling study rationalizes the surpassed *in vitro* activity of compound **5m** over **5h** against COX-2 enzyme ( $IC_{50}$  = 87.74 and 166.5 nM, respectively).

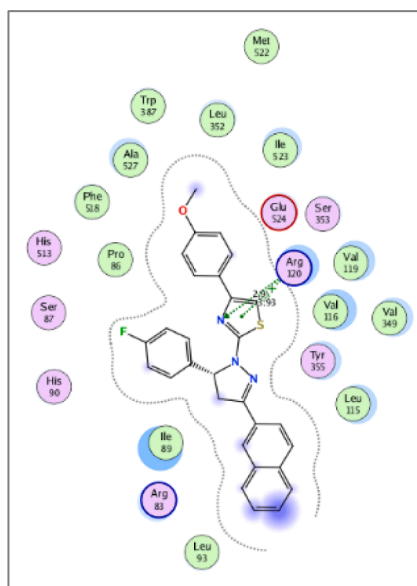
### 2.4. In vivo pharmacokinetic study

The bioanalytical technique is essential for monitoring therapy, assessing adherence to treatment, adjusting dosage, and studying the pharmacokinetics of medications [57]. Since compound **5m** showed some difficulties to be detected in mass spectroscopy, derivative **5d** was then picked out to perform the pharmacokinetic study as a potent analgesic (% potency = 120 %) and anti-inflammatory agent (% edema inhibition after 3 h = 75.15 %) that revealed moderate ulcer index (8.20). Thus, a sensitive and accurate UPLC-MS/MS method was developed for the simultaneous estimation of the synthesized pyrazole derivatives **5d** and **5h** in rat plasma using 3-(4-fluorophenyl)-1-

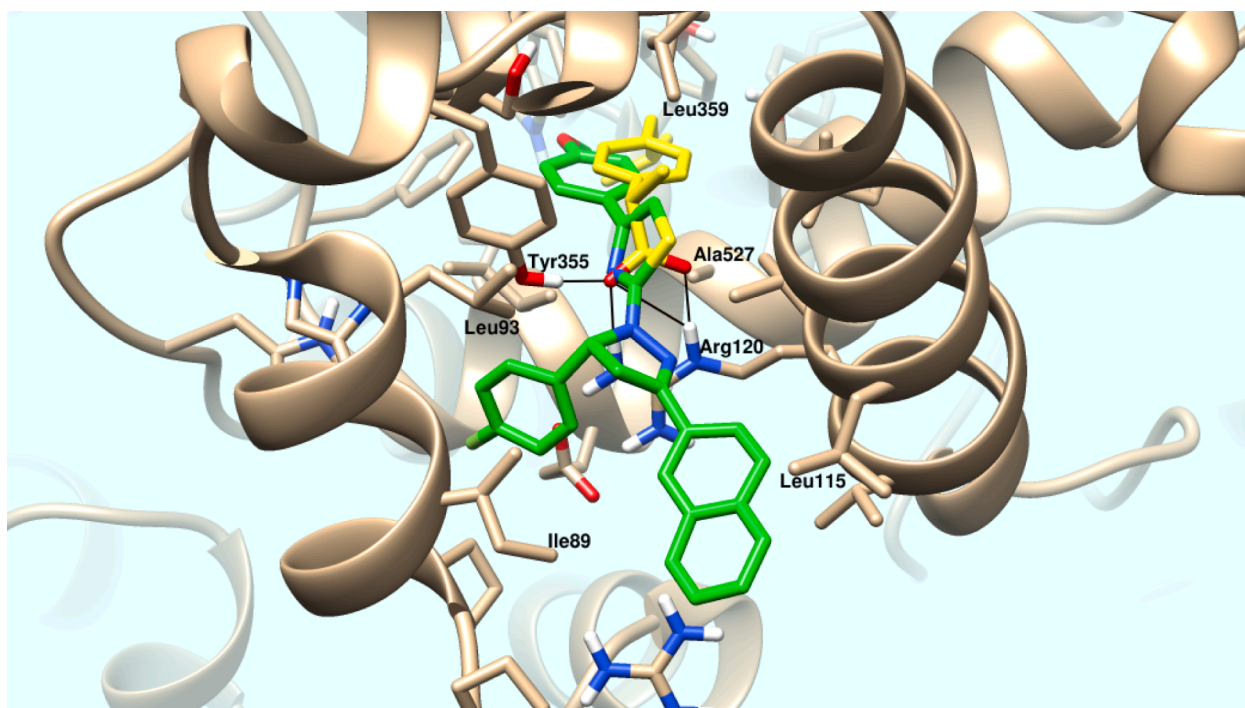
(naphthalen-2-yl)prop-2-en-1-one (XI) as internal standard (IS). Compounds **5d** and **5h** were extracted from rat plasma by liquid–liquid extraction using diethyl ether. For the detailed information regarding the method development and validation stages and results see [Supplementary Material \(Figure 12S-15-S, Tables 1S-5S\)](#).

The developed method was applied in preclinical *in vivo* pharmacokinetic study for the determination of plasma levels of the newly synthesized compounds **5d** and **5h** in rats after single subcutaneous dose

(10 mg/kg). Profiles of the plasma concentration vs. time of compounds **5d** and **5h** are shown in [Fig. 5](#). Pharmacokinetic parameters were recorded in [Table 5](#). The two compounds showed good pharmacokinetic parameters with maximum concentration in plasma ( $C_{max}$ , 1130.56 and 38.501 ng/mL) was achieved at 6 and 2 h for **5d** and **5h** respectively. The half-life ( $t_{1/2}$ ) of compound **5d** was 6.49 h. Additionally, compound **5h** expressed an excellent profile with half-life > 21 h, while the  $AUC_{0-\infty}$  was found 8591.40 and 4910.04 ng h/mL for compounds

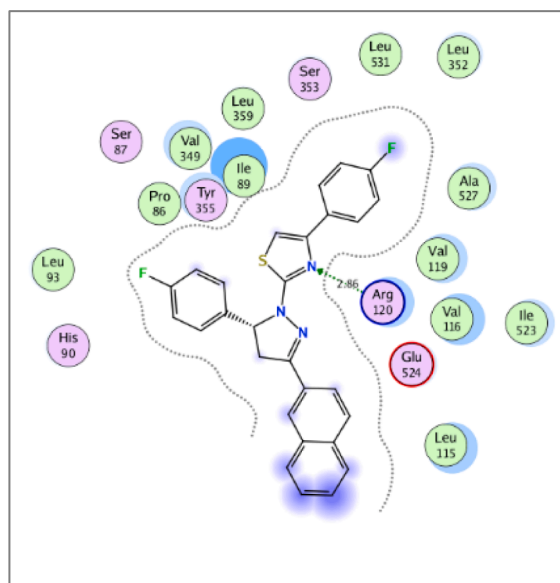


(A)

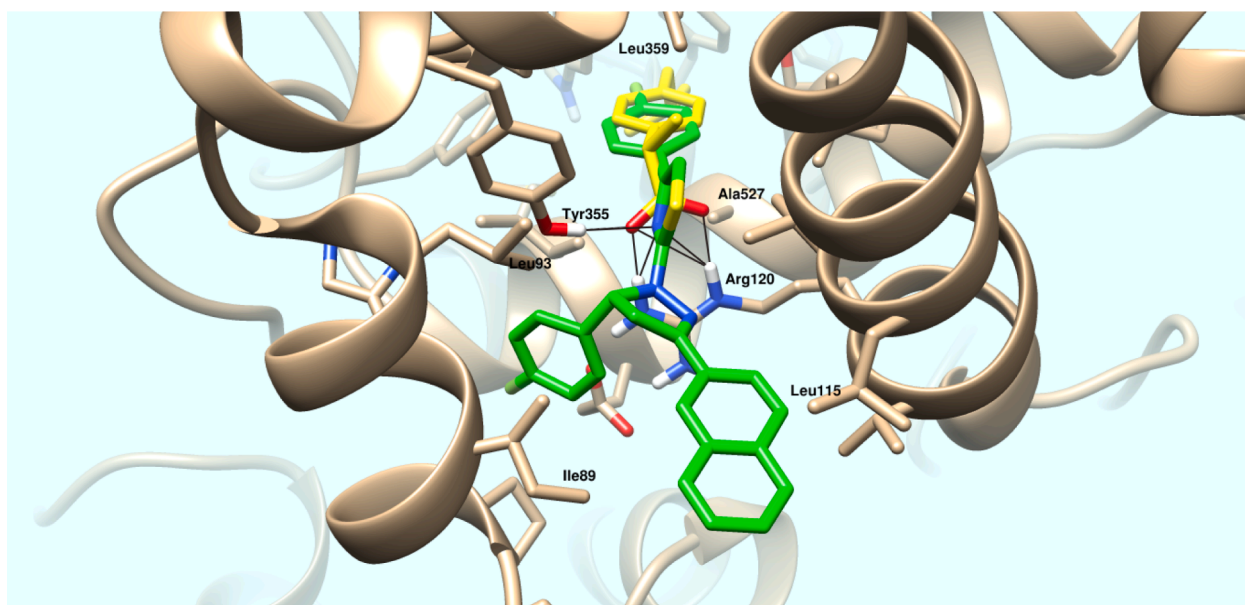


(B)

**Fig. 3.** Modeling of compound **5h** (A; 2D diagram and B; 3D overlay representation) and compound **5m** (C; 2D diagram and D; 3D overlay representation) into the active site of COX-1 (PDB ID: 1EQG). Compounds **5h,m** are colored green and the co-crystallized ligand Ibuprofen is colored yellow (Distances in Å). (For interpretation of the references to colour in this figure legend, the reader is referred to the web version of this article.)



(C)



(D)

Fig. 3. (continued).

**5d** and **5h**, respectively.

The described UPLC-MS/MS was an accurate, sensitive, selective, and fast technique with a run time not exceeding 6.30 min. The developed and validated methodology was proved useful for the simultaneous estimation of the two newly synthesized compounds **5d** and **5h** in rat plasma using the synthesized intermediate **XI** as IS. Sample preparation was conducted using liquid-liquid extraction with adequate recovery and the lower limit of quantification (LLOQ) was sufficiently low to estimate the mentioned compounds in plasma at a concentration as low as 20 ng/mL. This estimation demonstrated good accuracy and precision, both within a single day and across multiple days. Hence, the present bioanalytical technique effectively anticipated the pharmacokinetic characteristics of the two substances. This information could be valuable in therapeutic monitoring and adjusting dosage levels of therapeutic agents.

### 3. Conclusion

In the present study, new pyrazole clubbed thiazole derivatives **5a-o** were prepared and evaluated for their analgesic activity. Eight compounds **5a**, **5c**, **5d**, **5e**, **5f**, **5h**, **5m**, and **5o** were found to be more potent than Indomethacin, thus they were evaluated for their anti-inflammatory activity, ulcerogenic potential along with their toxicological studies. They exhibited good to moderate activity in form of % edema inhibition after 2 and 3 h of treatment, in comparison with Indomethacin. Moreover, compounds **5e**, **5h**, and **5m** displayed the lowest ulcerogenic effect, as indicated from their ulcer indices, as well as a high safety margin. Taking in consideration the whole conducted biological tests, the obtained results identified compounds **5h** and **5m** as the most promising agents. They revealed promising inhibitory activity against COX-1 ( $IC_{50}$  = 38.76 and 166.5 nM, respectively) and COX-2



( $IC_{50}$  = 179.70 and 87.7 nM, respectively). Additionally, the performed docking studies revealed a well accommodation of both compounds within COX-1 and COX-2 active site. Relying on the participation of pyrazole clubbed thiazole core in several binding. interactions, compound **5h** showed a preferential binding within COX-1 active site with Arg120 amino-acid by an additional arene-cation interaction to hydrogen bonding. Compound **5m** pyrazole clubbed thiazole moiety revealed three hydrogen bonding interactions with Val509, Ser516 and Leu517 residues along with different orientation of naphthalene side-chain. The docking studies of both compounds were found augmenting the exhibited inhibitory activity against COX-1 and COX-2 isozymes, which illustrate the promising COX modulation of the elucidated hybrid in replacing the carboxylic acid and sulfonamide function groups. Finally, a promising LC-MS/MS method for **5d** and **5h** quantification in rat plasma was developed and validated. The method was shown to be

simple, sensitive, and specific. The pharmacophoric hybridization strategy adopted in the designed compounds was shown to be successful and fruitful. Compounds **5h** and **5m** could be used efficiently as a starting point for further exploration and development of a new class of anti-inflammatory agents that are deviod from sulfonamide and carboxylic acid functionalities.

## 4. Experimental

### 4.1. Chemistry

All reagents and solvents were obtained from commercial suppliers. Further details regarding the used instrumentations and techniques (Melting point, Elemental Microanalyses,  $^1H$  NMR and  $^{13}C$  NMR Spectra and microanalytical experiments) are presented in [Supplementary](#)

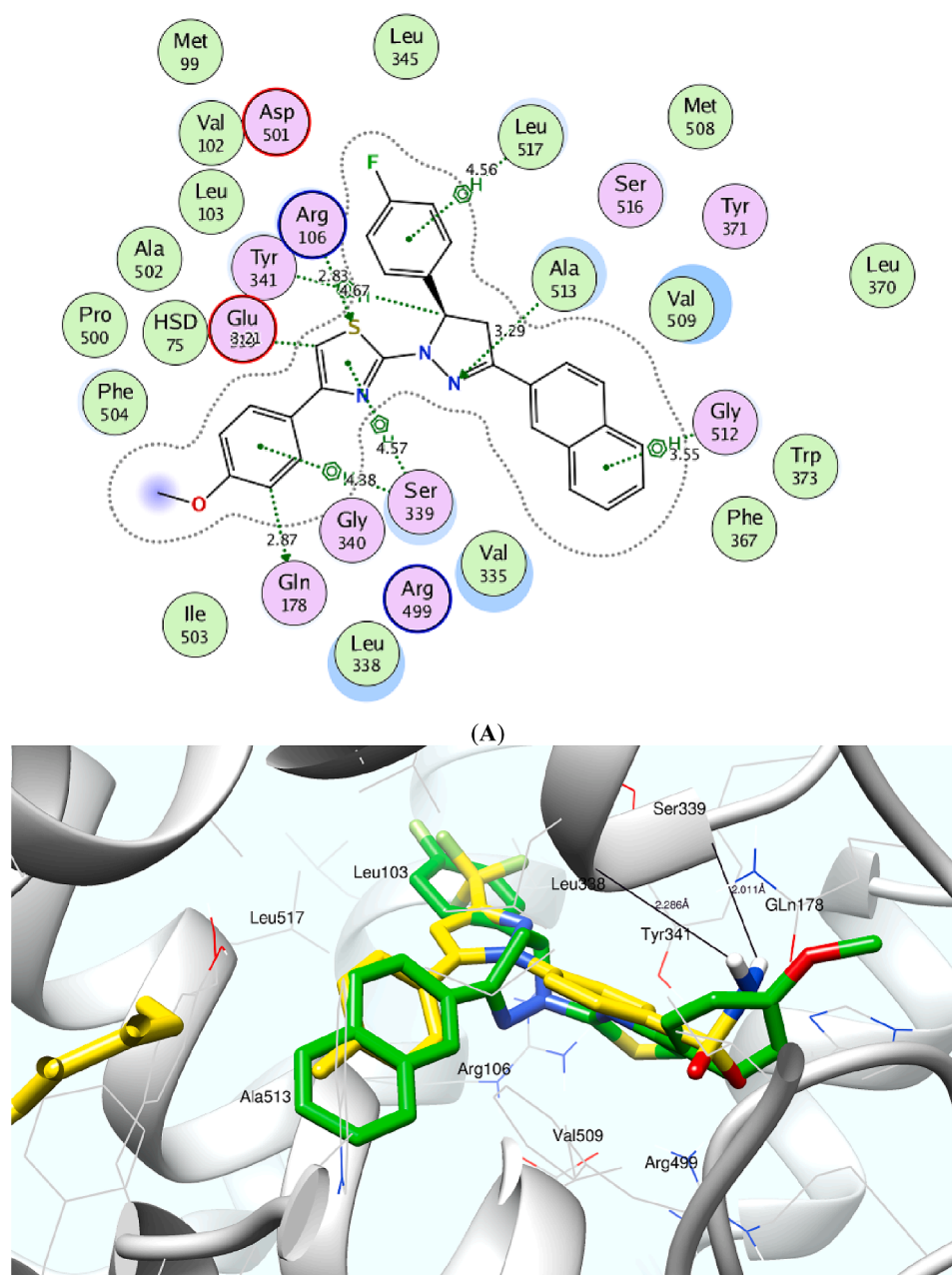
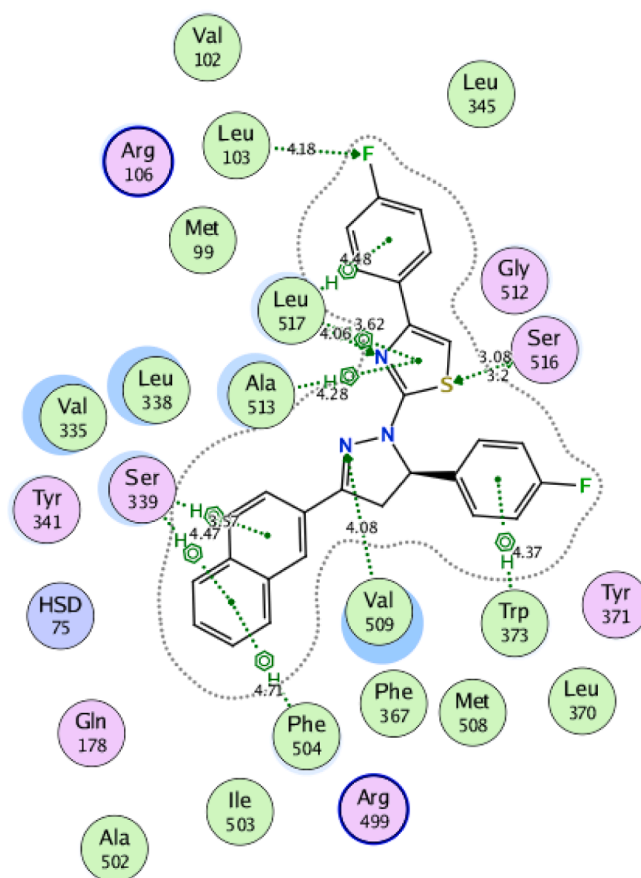
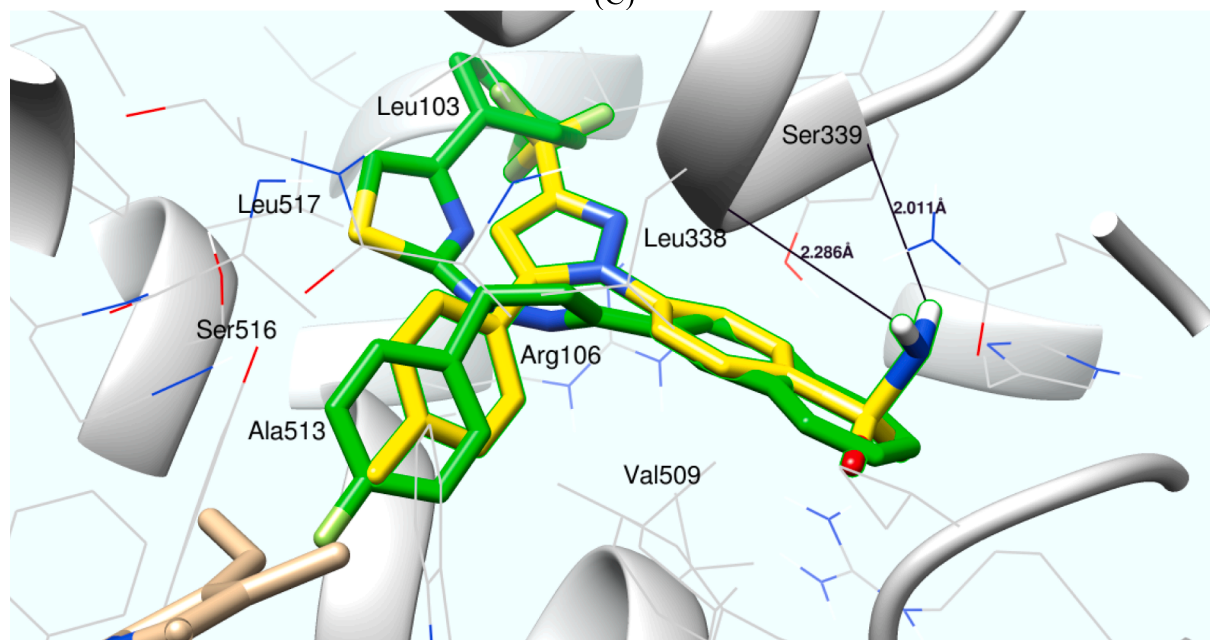


**Fig. 4.** Modeling of compound **5h** (A; 2D diagram and B; 3D overlay representation) and compound **5m** (C; 2D diagram and D; 3D overlay representation) into the active site of COX-2 (PDB ID: 3LN1). Compounds **5h,m** are colored green and the co-crystallized ligand Celecoxib I is colored yellow (Distances in Å). (For interpretation of the references to colour in this figure legend, the reader is referred to the web version of this article.)

(B)



(C)



(D)

Fig. 4. (continued).

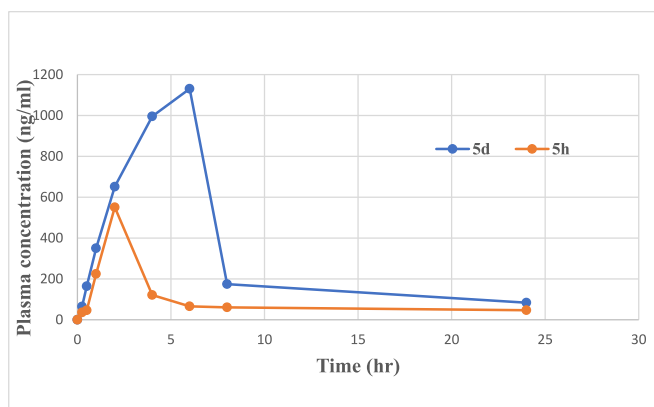


Fig. 5. Mean plasma concentration-time profiles of **5d** and **5h** after a single subcutaneous dose of 10 mg/kg in rats.

Table 5

Pharmacokinetic parameters of **5d** and **5h** after subcutaneous dose of 10 mg/Kg to rats.

Pharmacokinetic parameters	5d	5h
C <sub>max</sub> (ng/mL)	1130.56	550.82
T <sub>max</sub> (h)	6	2
t <sub>1/2</sub> (h)	6.490	38.501
AUC <sub>0-48</sub> (ng.h/mL)	7808.221	2314.925
AUC <sub>0-∞</sub> (ng.h/mL)	8591.405	4910.049
CL (mL.h/kg)	1.163	2.036

C<sub>max</sub>=maximum concentration in plasma, T<sub>max</sub> = time to maximum plasma concentration, t<sub>1/2</sub> = half-life of drug elimination, AUC = area under the plasma concentration-time curve from zero hour to 48 h, AUC<sub>0-∞</sub> = area under the plasma concentration-time curve from zero hour to infinite time and CL = clearance rate.

**material.** Compounds **2a-e** [37], **3a-d** [37] and **4a-c** [37] were synthesized according to the reported procedures.

#### 4.1.1. Synthesis of 5-(4-(dimethylamino)phenyl)-3-(naphthalen-2-yl)-4,5-dihydro-1H-pyrazole-1-carbothioamide (**3e**)

To a stirred solution of the chalcone derivative **2e** (0.5 g, 1.7 mmol) in hot absolute ethanol (5 mL), thiosemicarbazide (0.17 g, 1.8 mmol) was added in the presence of sodium hydroxide (0.15 g, 3.75 mmol). The reaction mixture was refluxed for 8 h. The solution was evaporated under *vacuum* and the residue obtained was washed with hot absolute ethanol and dried to give orange crystals; yield 60 %; m.p. 250–252 °C; IR (KBr, cm<sup>-1</sup>): 3035 (CH aromatic), 2954, 2889 (CH aliphatic), 3406, 3263 (NH<sub>2</sub>), 1454, 1357 (C=C), 1192 (C=S); <sup>1</sup>H NMR (DMSO): δ 2.84 (s, 6H, N(CH<sub>3</sub>)<sub>2</sub>), 3.24 (dd, 1H, *J* = 17.78, 2.9, CH<sub>2</sub>), 3.91 (dd, 1H, *J* = 17.74, 11.18, CH<sub>2</sub>), 5.86 (dd, 1H, *J* = 11.04, 2.72, CH), 6.65 (d, 2H, *J* = 8.72, aromatic H), 6.99 (d, 2H, *J* = 8.64, aromatic H), 7.55–7.60 (m, 2H, aromatic H), 7.94–7.99 (m, 5H, aromatic H), 8.23 (s, 2H, NH<sub>2</sub>); <sup>13</sup>C NMR (DMSO): δ 40.68 (N(CH<sub>3</sub>)<sub>2</sub>), 42.82 (pyrazoline CH<sub>2</sub>), 63.04 (pyrazoline CH), 112.88, 124.09, 126.68, 127.29, 127.83, 128.20, 128.39, 128.60, 128.89, 129.21, 131.09, 133.16, 134.18, 150.03, 155.55; Anal. Calcd. For C<sub>22</sub>H<sub>22</sub>N<sub>4</sub>S (374.51): C, 70.56; H, 5.92; N, 14.96. Found: C, 70.50; H, 5.93; N, 14.95.

#### 4.1.2. General procedures for synthesis of 4-(4-Substitutedphenyl)-2-(5-(4-un/substitutedphenyl)-3-(naphthalen-2-yl)-4,5-dihydro-1H-pyrazol-1-yl)thiazole (**5a-o**)

A mixture of equimolar amounts of 5-(4-substituted phenyl)-3-(naphthalen-2-yl)-4,5-dihydro-1H-pyrazole-1-carbothioamide **3a-e** (0.8 mmol) and the appropriate 2-bromo-1-(4-substitutedphenyl)ethan-1-one **4a-c** (0.8 mmol) in absolute ethanol (20 mL) was heated under reflux for 2–6 h. The obtained solid was filtered on hot, washed with hot

ethanol and dried.

**4.1.2.1. 4-(4-Chlorophenyl)-2-(3-(naphthalen-2-yl)-5-phenyl-4,5-dihydro-1H-pyrazol-1-yl)thiazole (**5a**).** Yellow solid; yield 73 %; m.p. 240–242 °C; IR (KBr, cm<sup>-1</sup>): 3059 (CH aromatic), 2954, 2912 (CH aliphatic), 1543, 1504 (C=C); <sup>1</sup>H NMR (CDCl<sub>3</sub>): δ 3.50 (dd, 1H, *J* = 17.36, 6.16, CH<sub>2</sub>), 4.03 (dd, 1H, *J* = 17.36, 11.88, CH<sub>2</sub>), 5.99 (s br., 1H, CH), 6.81 (s, 1H, aromatic H), 7.29–7.33 (m, 3H, aromatic H), 7.39 (t, 2H, *J* = 7.5, aromatic H), 7.49–7.58 (m, 4H, aromatic H), 7.63 (d, 2H, *J* = 8.48, aromatic H), 7.86–7.96 (m, 4H, aromatic H), 8.14 (dd, 1H, *J* = 8.60, 1.32, aromatic H); <sup>13</sup>C NMR (CDCl<sub>3</sub>): δ 43.87 (pyrazoline CH<sub>2</sub>), 64.89 (pyrazoline CH), 103.63, 123.44, 126.65, 126.87, 127.21, 127.39, 127.54, 127.91, 128.18, 128.40, 128.49, 128.64, 128.74, 128.94, 129.06, 131.55, 133.03, 133.96, 134.24, 165.01; Anal. Calcd. for C<sub>28</sub>H<sub>20</sub>ClN<sub>3</sub>S (466.00): C, 72.17; H, 4.33; N, 9.02. Found: C, 71.86; H, 4.50; N, 9.27.

**4.1.2.2. 4-(4-Chlorophenyl)-2-(5-(4-chlorophenyl)-3-(naphthalen-2-yl)-4,5-dihydro-1H-pyrazol-1-yl)thiazole (**5b**).** Light yellow solid; yield 75 %; m.p. 260–262 °C; IR (KBr, cm<sup>-1</sup>): 3055 (CH aromatic), 2958, 2900 (CH aliphatic), 1543, 1504 (C=C); <sup>1</sup>H NMR (DMSO): δ 3.49 (dd, 1H, *J* = 17.74, 6.42, CH<sub>2</sub>), 4.16 (dd, 1H, *J* = 17.78, 11.94, CH<sub>2</sub>), 5.76 (dd, 1H, *J* = 11.68, 6.24, CH), 7.42–7.50 (m, 7H, aromatic H), 7.59 (t, 2H, *J* = 4.10, aromatic H), 7.74 (d, 2H, *J* = 8.12, aromatic H), 7.97–8.08 (m, 4H, aromatic H), 8.20 (s, 1H, aromatic H); <sup>13</sup>C NMR (DMSO): δ 43.42 (pyrazoline CH<sub>2</sub>), 64.10 (pyrazoline CH), 105.82, 123.50, 127.36, 127.55, 127.63, 127.71, 128.23, 128.85, 128.90, 129.05, 129.13, 132.46, 132.57, 133.26, 133.72, 133.96, 141.14, 149.71, 153.60, 164.78; Anal. Calcd. for C<sub>28</sub>H<sub>19</sub>Cl<sub>2</sub>N<sub>3</sub>S (500.44): C, 67.20; H, 3.83; N, 8.40. Found: C, 67.43; H, 4.01; N, 8.64.

**4.1.2.3. 4-(4-Chlorophenyl)-2-(5-(4-fluorophenyl)-3-(naphthalen-2-yl)-4,5-dihydro-1H-pyrazol-1-yl)thiazole (**5c**).** Buff solid; yield 93 %; m.p. 242–244 °C; IR (KBr, cm<sup>-1</sup>): 3055 (CH aromatic), 2958, 2904 (CH aliphatic), 1546, 1508 (C=C); <sup>1</sup>H NMR (CDCl<sub>3</sub>): δ 3.45 (dd, 1H, *J* = 17.34, 6.62, CH<sub>2</sub>), 4.02 (dd, 1H, *J* = 17.34, 11.94, CH<sub>2</sub>), 5.78 (dd, 1H, *J* = 11.08, 6.44, CH), 6.84 (s, 1H, aromatic H), 7.05–7.1 (m, 2H, aromatic H), 7.31 (d, 2H, *J* = 8.56, aromatic H), 7.44 (dd, 2H, *J* = 5.28, 8.68, aromatic H), 7.54–7.57 (m, 2H, aromatic H), 7.62 (d, 2H, *J* = 8.56, aromatic H), 7.86–7.95 (m, 4H, aromatic H), 8.14 (dd, 1H, *J* = 8.60, 1.6, aromatic H); <sup>13</sup>C NMR (CDCl<sub>3</sub>): δ 43.62 (pyrazoline CH<sub>2</sub>), 64.19 (pyrazoline CH), 103.82, 115.63, 115.85, 123.39, 126.84, 126.87, 127.30, 127.92, 128.39, 128.42, 128.47, 128.61, 128.69, 133.06, 133.60, 134.13, 137.00, 149.30, 153.08, 161.15, 163.60, 164.94; Anal. Calcd. For C<sub>28</sub>H<sub>19</sub>ClFN<sub>3</sub>S (483.99): C, 69.49; H, 3.96; N, 8.68. Found: C, 69.70; H, 3.85; N, 8.89.

**4.1.2.4. 4-(4-Chlorophenyl)-2-(5-(4-methoxyphenyl)-3-(naphthalen-2-yl)-4,5-dihydro-1H-pyrazol-1-yl)thiazole (**5d**).** Yellow solid; yield 72 %; m.p. 228–230 °C; IR (KBr, cm<sup>-1</sup>): 3055 (CH aromatic), 2958, 2904 (CH aliphatic), 1546, 1516 (C=C); <sup>1</sup>H NMR (DMSO): δ 3.47 (dd, 1H, *J* = 17.74, 6.18, CH<sub>2</sub>), 3.72 (s, 3H, OCH<sub>3</sub>), 4.11 (dd, 1H, *J* = 17.74, 11.86, CH<sub>2</sub>), 5.69 (dd, 1H, *J* = 11.80, 6.16, CH), 6.92 (d, 2H, *J* = 8.72, aromatic H), 7.36 (d, 2H, *J* = 8.72, aromatic H), 7.43 (t, 3H, *J* = 7.44, aromatic H), 7.57–7.60 (m, 2H, aromatic H), 7.77 (d, 2H, *J* = 8.56, aromatic H), 7.96–8.02 (m, 3H, aromatic H), 8.06 (dd, 1H, *J* = 8.66, 1.50, aromatic H), 8.20 (s, 1H, aromatic H); <sup>13</sup>C NMR (DMSO): δ 43.41 (pyrazoline CH<sub>2</sub>), 55.51 (OCH<sub>3</sub>), 64.21 (pyrazoline CH), 105.56, 114.37, 123.51, 127.33, 127.42, 127.67, 128.22, 128.49, 128.81, 128.88, 129.02, 132.41, 133.30, 133.83, 133.92, 134.08, 149.74, 153.45, 159.13, 164.75; Anal. Calcd. For C<sub>29</sub>H<sub>22</sub>ClN<sub>3</sub>OS (496.03): C, 70.22; H, 4.47; N, 8.47. Found: C, 70.08; H, 4.65; N, 8.69.

**4.1.2.5. 4-(1-(4-(4-Chlorophenyl)thiazol-2-yl)-3-(naphthalen-2-yl)-4,5-dihydro-1H-pyrazol-5-yl)-N,N-dimethylaniline (**5e**).** Dark yellow solid;

yield 67 %; m.p. 278–280 °C; IR (KBr,  $\text{cm}^{-1}$ ): 3051 (CH aromatic), 2889, 2854 (CH aliphatic), 1546, 1446 ( $\text{C}=\text{C}$ );  $^1\text{H}$  NMR ( $\text{CDCl}_3$ ):  $\delta$  2.93 (s, 6H,  $-\text{N}(\text{CH}_3)_2$ ), 3.49 (dd, 1H,  $J = 17.40, 6.44$ ,  $\text{CH}_2$ ), 3.97 (dd, 1H,  $J = 17.28, 11.88$ ,  $\text{CH}_2$ ), 5.64 (dd, 1H,  $J = 11.88, 6.32$ , CH), 6.72 (d, 2H,  $J = 8.68$ , aromatic H), 6.82 (s, 1H, aromatic H), 7.01–7.09 (m, 1H, aromatic H), 7.31 (q, 3H,  $J = 7.36$ , aromatic H), 7.53–7.55 (m, 2H, aromatic H), 7.69 (d, 2H,  $J = 8.48$ , aromatic H), 7.87–7.95 (m, 4H, aromatic H), 8.16 (dd, 1H,  $J = 8.58, 1.22$ , aromatic H);  $^{13}\text{C}$  NMR ( $\text{CDCl}_3$ ):  $\delta$  40.54 ( $\text{N}(\text{CH}_3)_2$ ), 43.17 (pyrazoline  $\text{CH}_2$ ), 64.43 (pyrazoline CH), 103.55, 112.45, 112.60, 123.53, 126.33, 126.64, 126.90, 127.03, 127.22, 127.41, 127.80, 127.88, 128.34, 128.40, 128.50, 129.21, 129.33, 132.92, 133.16, 133.91, 151.81; Anal. Calcd. For  $\text{C}_{30}\text{H}_{25}\text{ClN}_4\text{S}$  (509.07): C, 70.78; H, 4.95; N, 11.01. Found: C, 70.94; H, 5.12; N, 11.23.

**4.1.2.6. 4-(4-Methoxyphenyl)-2-(3-(naphthalen-2-yl)-5-phenyl-4,5-dihydro-1H-pyrazol-1-yl)thiazole (5f).** Buff solid; yield 85 %; m.p. 255–257 °C; IR (KBr,  $\text{cm}^{-1}$ ): 3028 (CH aromatic), 2966, 2939 (CH aliphatic), 1543, 1489 ( $\text{C}=\text{C}$ );  $^1\text{H}$  NMR (DMSO):  $\delta$  3.47 (dd, 1H,  $J = 17.74, 6.46$ ,  $\text{CH}_2$ ), 3.77 (s, 3H,  $\text{OCH}_3$ ), 4.15 (dd, 1H,  $J = 17.70, 11.94$ ,  $\text{CH}_2$ ), 5.74 (dd, 1H,  $J = 11.90, 6.42$ , CH), 6.91 (d, 2H,  $J = 8.84$ , aromatic H), 7.18 (s, 1H, aromatic H), 7.27–7.31 (m, 1H, aromatic H), 7.39 (t, 2H,  $J = 7.6$ , aromatic H), 7.44 (d, 2H,  $J = 7.24$ , aromatic H), 7.57–7.60 (m, 2H, aromatic H), 7.64 (d, 2H,  $J = 8.76$ , aromatic H), 7.96–8.02 (m, 3H, aromatic H), 8.06 (dd, 1H,  $J = 8.66, 1.46$ , aromatic H), 8.20 (s, 1H, aromatic H);  $^{13}\text{C}$  NMR (DMSO):  $\delta$  43.54 (pyrazoline  $\text{CH}_2$ ), 55.56 ( $\text{OCH}_3$ ), 64.78 (pyrazoline CH), 102.69, 114.33, 123.49, 127.09, 127.31, 127.37, 127.64, 127.82, 128.01, 128.21, 128.82, 128.88, 129.05, 133.29, 133.89, 142.38, 150.82, 153.15, 159.25, 164.60; MS  $m/z$ : 461.66 ( $\text{M}^+$ , 23.54 %), 395.55 (100 %). Anal. Calcd. For  $\text{C}_{29}\text{H}_{23}\text{N}_3\text{OS}$  (461.58): C, 75.46; H, 5.02; N, 9.10. Found: C, 75.54; H, 4.73; N, 8.98.

**4.1.2.7. 4-(4-Methoxyphenyl)-2-(5-(4-chlorophenyl)-3-(naphthalen-2-yl)-4,5-dihydro-1H-pyrazol-1-yl)thiazole (5g).** Light yellow solid; yield 93 %; m.p. 233–235 °C; IR (KBr,  $\text{cm}^{-1}$ ): 3051 (CH aromatic), 2935, 2904 (CH aliphatic), 1543, 1489 ( $\text{C}=\text{C}$ );  $^1\text{H}$  NMR (DMSO):  $\delta$  3.47 (dd, 1H,  $J = 17.76, 6.68$ ,  $\text{CH}_2$ ), 3.77 (s, 3H,  $\text{OCH}_3$ ), 4.14 (dd, 1H,  $J = 17.74, 11.94$ ,  $\text{CH}_2$ ), 5.73 (dd, 1H,  $J = 11.90, 6.66$ , CH), 6.92 (d, 2H,  $J = 8.8$ , aromatic H), 7.19 (s, 1H, aromatic H), 7.43 (q, 4H,  $J = 8.16$ , aromatic H), 7.57–7.60 (m, 2H, aromatic H), 7.65 (d, 2H,  $J = 8.76$ , aromatic H), 7.96–8.02 (m, 3H, aromatic H), 8.05 (dd, 1H,  $J = 8.66, 1.38$ , aromatic H), 8.19 (s, 1H, aromatic H);  $^{13}\text{C}$  NMR (DMSO):  $\delta$  43.38 (pyrazoline  $\text{CH}_2$ ), 55.57 ( $\text{OCH}_3$ ), 64.18 (pyrazoline CH), 102.85, 114.37, 123.50, 127.30, 127.35, 127.46, 127.68, 127.76, 128.23, 128.83, 128.88, 128.94, 129.03, 129.15, 132.51, 133.28, 133.92, 141.33, 150.81, 153.28, 159.28, 164.58; Anal. Calcd. For  $\text{C}_{29}\text{H}_{22}\text{ClN}_3\text{OS}$  (496.03): C, 70.22; H, 4.47; N, 8.47. Found: C, 70.43; H, 4.60; N, 8.65.

**4.1.2.8. 4-(4-Methoxyphenyl)-2-(5-(4-fluorophenyl)-3-(naphthalen-2-yl)-4,5-dihydro-1H-pyrazol-1-yl)thiazole (5h).** Yellow solid; yield 96 %; m.p. 253–255 °C; IR (KBr,  $\text{cm}^{-1}$ ): 3008 (CH aromatic), 2966, 2935 (CH aliphatic), 1546, 1512 ( $\text{C}=\text{C}$ );  $^1\text{H}$  NMR (DMSO):  $\delta$  3.48 (dd, 1H,  $J = 17.74, 6.70$ ,  $\text{CH}_2$ ), 3.77 (s, 3H,  $\text{OCH}_3$ ), 4.14 (dd, 1H,  $J = 17.76, 11.92$ ,  $\text{CH}_2$ ), 5.73 (dd, 1H,  $J = 11.86, 6.70$ , CH), 6.92 (d, 2H,  $J = 8.88$ , aromatic H), 7.18–7.24 (m, 3H, aromatic H), 7.49 (dd, 2H,  $J = 8.64, 5.46$ , aromatic H), 7.57–7.60 (m, 2H, aromatic H), 7.65 (d, 2H,  $J = 8.80$ , aromatic H), 7.96–8.02 (m, 3H, aromatic H), 8.06 (dd, 1H,  $J = 8.62, 1.54$ , aromatic H), 8.19 (s, 1H, aromatic H);  $^{13}\text{C}$  NMR (DMSO):  $\delta$  43.45 (pyrazoline  $\text{CH}_2$ ), 55.57 ( $\text{OCH}_3$ ), 64.19 (pyrazoline CH), 102.79, 114.36, 115.68, 115.90, 123.51, 127.30, 127.43, 127.65, 127.81, 128.23, 128.81, 128.88, 129.00, 129.26, 129.34, 133.29, 133.92, 138.51, 150.83, 153.22, 159.27, 160.72, 163.14, 164.62; Anal. Calcd. For  $\text{C}_{29}\text{H}_{22}\text{FN}_3\text{OS}$  (479.57): C, 72.63; H, 4.62; N, 8.76. Found: C, 72.51; H, 4.80; N, 9.03.

**4.1.2.9. 4-(4-Methoxyphenyl)-2-(5-(4-methoxyphenyl)-3-(naphthalen-2-yl)-4,5-dihydro-1H-pyrazol-1-yl)thiazole (5i).** Dark yellow solid; yield 90 %; m.p. 222–224 °C; IR (KBr,  $\text{cm}^{-1}$ ): 3035 (CH aromatic), 2954, 2935 (CH aliphatic), 1546, 1512 ( $\text{C}=\text{C}$ );  $^1\text{H}$  NMR (DMSO):  $\delta$  3.46 (dd, 1H,  $J = 17.72, 6.28$ ,  $\text{CH}_2$ ), 3.72 (s, 3H,  $\text{OCH}_3$ ), 3.77 (s, 3H,  $\text{OCH}_3$ ), 4.10 (dd, 1H,  $J = 17.70, 11.90$ ,  $\text{CH}_2$ ), 5.68 (dd, 1H,  $J = 11.86, 6.26$ , CH), 6.92 (dd, 4H,  $J = 8.76, 1.56$ , aromatic H), 7.16 (s, 1H, aromatic H), 7.36 (d, 2H,  $J = 8.72$ , aromatic H), 7.57–7.60 (m, 2H, aromatic H), 7.68 (d, 2H,  $J = 8.80$ , aromatic H), 7.96–8.02 (m, 3H, aromatic H), 8.06 (dd, 1H,  $J = 8.66, 1.54$ , aromatic H), 8.19 (s, 1H, aromatic H);  $^{13}\text{C}$  NMR (DMSO):  $\delta$  43.34 (pyrazoline  $\text{CH}_2$ ), 55.50 ( $\text{OCH}_3$ ), 55.56 ( $\text{OCH}_3$ ), 64.23 (pyrazoline CH), 102.58, 114.34, 123.47, 127.33, 127.63, 127.85, 128.21, 128.48, 128.81, 128.87, 129.10, 133.29, 133.87, 134.24, 150.84, 153.11, 159.08, 159.24, 164.57; Anal. Calcd. For  $\text{C}_{30}\text{H}_{25}\text{N}_3\text{O}_2\text{S}$  (491.61): C, 73.30; H, 5.13; N, 8.55. Found: C, 73.49; H, 5.40; N, 8.79.

**4.1.2.10. 4-(1-(4-(4-Methoxyphenyl)thiazol-2-yl)-3-(naphthalen-2-yl)-4,5-dihydro-1H-pyrazol-5-yl)-N,N-dimethylaniline (5j).** Buff solid; yield 82 %; m.p. 268–270 °C; IR (KBr,  $\text{cm}^{-1}$ ): 3008 (CH aromatic), 2966, 2935 (CH aliphatic), 1550, 1527 ( $\text{C}=\text{C}$ );  $^1\text{H}$  NMR (DMSO):  $\delta$  2.85 (s, 6H,  $\text{N}(\text{CH}_3)_2$ ), 3.44 (dd, 1H,  $J = 17.40, 4.92$ ,  $\text{CH}_2$ ), 3.77 (s, 3H,  $\text{OCH}_3$ ), 4.05 (dd, 1H,  $J = 17.12, 12.12$ ,  $\text{CH}_2$ ), 5.63 (dd, 1H,  $J = 10.74, 5.38$ , CH), 6.68 (d, 2H,  $J = 8.04$ , aromatic H), 6.93 (d, 2H,  $J = 8.12$ , aromatic H), 7.14 (s, 1H, aromatic H), 7.24 (d, 2H,  $J = 8.12$ , aromatic H), 7.58 (s, 2H, aromatic H), 7.71 (d, 2H,  $J = 8.08$ , aromatic H), 7.99–8.08 (m, 4H, aromatic H), 8.18 (s, 1H, aromatic H);  $^{13}\text{C}$  NMR (DMSO):  $\delta$  40.54 ( $\text{N}(\text{CH}_3)_2$ ), 43.07 (pyrazoline  $\text{CH}_2$ ), 55.57 ( $\text{OCH}_3$ ), 64.32 (pyrazoline CH), 102.42, 112.69, 114.34, 123.49, 127.20, 127.36, 127.58, 128.02, 128.21, 128.79, 128.86, 129.24, 133.33, 133.85, 150.35, 150.86, 153.05, 159.23, 159.45, 164.51; MS  $m/z$ : 504.03 ( $\text{M}^+$ , 39.66 %), 139.23 (100 %). Anal. Calcd. For  $\text{C}_{31}\text{H}_{28}\text{N}_4\text{OS}$  (504.65): C, 73.78; H, 5.59; N, 11.10. Found: C, 74.04; H, 5.71; N, 11.36.

**4.1.2.11. 4-(4-Fluorophenyl)-2-(3-(naphthalen-2-yl)-5-phenyl-4,5-dihydro-1H-pyrazol-1-yl)thiazole (5k).** Yellow solid; yield 83 %; m.p. 248–250 °C; IR (KBr,  $\text{cm}^{-1}$ ): 3032 (CH aromatic), 2970, 2904 (CH aliphatic), 1550, 1485 ( $\text{C}=\text{C}$ );  $^1\text{H}$  NMR (DMSO):  $\delta$  3.47 (dd, 1H,  $J = 17.80, 5.60$ ,  $\text{CH}_2$ ), 4.15 (dd, 1H,  $J = 17.14, 12.16$ ,  $\text{CH}_2$ ), 5.73 (dd, 1H,  $J = 10.92, 5.92$ , CH), 7.19 (t, 2H,  $J = 8.16$ , aromatic H), 7.29–7.45 (m, 6H, aromatic H), 7.58 (s, 2H, aromatic H), 7.76 (s, 2H, aromatic H), 7.99–8.08 (m, 4H, aromatic H), 8.19 (s, 1H, aromatic H);  $^{13}\text{C}$  NMR (DMSO):  $\delta$  43.58 (pyrazoline  $\text{CH}_2$ ), 64.72 (pyrazoline CH), 104.57, 115.71, 115.92, 123.48, 127.05, 127.33, 127.44, 127.67, 127.88, 127.96, 128.05, 128.21, 128.82, 128.88, 128.96, 129.08, 131.54, 133.27, 133.91, 142.27, 149.91, 153.38, 164.77; Anal. Calcd. For  $\text{C}_{28}\text{H}_{20}\text{FN}_3\text{S}$  (449.55): C, 74.81; H, 4.48; N, 9.35. Found: C, 74.59; H, 4.67; N, 9.54.

**4.1.2.12. 4-(4-Fluorophenyl)-2-(5-(4-chlorophenyl)-3-(naphthalen-2-yl)-4,5-dihydro-1H-pyrazol-1-yl)thiazole (5l).** Light yellow solid; yield 90 %; m.p. 197–199 °C; IR (KBr,  $\text{cm}^{-1}$ ): 3055 (CH aromatic), 2954, 2916 (CH aliphatic), 1543, 1485 ( $\text{C}=\text{C}$ );  $^1\text{H}$  NMR ( $\text{CDCl}_3$ ):  $\delta$  3.42 (dd, 1H,  $J = 17.32, 6.84$ ,  $\text{CH}_2$ ), 4.02 (dd, 1H,  $J = 17.34, 12.02$ ,  $\text{CH}_2$ ), 5.68 (dd, 1H,  $J = 12.00, 6.84$ , CH), 6.80 (s, 1H, aromatic H), 7.04 (t, 2H,  $J = 8.72$ , aromatic H), 7.35 (q, 4H,  $J = 9.96$ , aromatic H), 7.52–7.57 (m, 2H, aromatic H), 7.64 (dd, 2H,  $J = 8.72, 5.48$ , aromatic H), 7.86–7.93 (m, 4H, aromatic H), 8.14 (dd, 1H,  $J = 8.62, 1.50$ , aromatic H);  $^{13}\text{C}$  NMR ( $\text{CDCl}_3$ ):  $\delta$  43.37 (pyrazoline  $\text{CH}_2$ ), 64.19 (pyrazoline CH), 103.13, 115.21, 115.43, 123.40, 126.48, 126.76, 127.10, 127.46, 127.54, 127.91, 128.04, 128.35, 128.54, 128.93, 131.22, 133.10, 133.52, 134.00, 140.32, 150.61, 151.66, 161.12, 163.57, 164.90; Anal. Calcd. For  $\text{C}_{28}\text{H}_{19}\text{ClFN}_3\text{S}$  (483.99): C, 69.49; H, 3.96; N, 8.68. Found: C, 69.78; H, 4.15; N, 8.89.



**4.1.2.13. 4-(4-Fluorophenyl)-2-(5-(4-fluorophenyl)-3-(naphthalen-2-yl)-4,5-dihydro-1H-pyrazol-1-yl)thiazole (5m).** Buff solid; yield 95 %; m.p. 202–204 °C; IR (KBr,  $\text{cm}^{-1}$ ): 3047 (CH aromatic), 2951, 2904 (CH aliphatic), 1550, 1508 (C=C);  $^1\text{H}$  NMR (DMSO):  $\delta$  3.49 (dd, 1H,  $J$  = 17.80, 6.64,  $\text{CH}_2$ ), 4.14 (dd, 1H,  $J$  = 17.76, 11.92,  $\text{CH}_2$ ), 5.74 (dd, 1H,  $J$  = 11.88, 6.60, CH), 7.18–7.23 (m, 4H, aromatic H), 7.34 (s, 1H, aromatic H), 7.49 (dd, 2H,  $J$  = 8.64, 5.48, aromatic H), 7.57–7.61 (m, 2H, aromatic H), 7.75 (dd, 2H,  $J$  = 8.74, 5.62, aromatic H), 7.96–8.02 (m, 3H, aromatic H), 8.06 (dd, 1H,  $J$  = 8.66, 1.42, aromatic H), 8.20 (s, 1H, aromatic H);  $^{13}\text{C}$  NMR (DMSO):  $\delta$  43.48 (pyrazoline  $\text{CH}_2$ ), 64.13 (pyrazoline CH), 104.69, 115.71, 115.92, 123.49, 127.34, 127.49, 127.68, 127.88, 127.96, 128.22, 128.82, 128.89, 128.93, 129.24, 129.32, 131.54, 133.27, 133.94, 138.42, 149.91, 153.45, 160.85, 163.15, 164.80; Anal. Calcd. For  $\text{C}_{28}\text{H}_{19}\text{F}_2\text{N}_3\text{S}$  (467.54): C, 71.93; H, 4.10; N, 8.99. Found: C, 72.09; H, 4.27; N, 9.21.

**4.1.2.14. 4-(4-Fluorophenyl)-2-(5-(4-methoxyphenyl)-3-(naphthalen-2-yl)-4,5-dihydro-1H-pyrazol-1-yl)thiazole (5n).** Dark yellow solid; yield 86 %; m.p. 228–230 °C; IR (KBr,  $\text{cm}^{-1}$ ): 3059 (CH aromatic), 2958, 2935 (CH aliphatic), 1550, 1516 (C=C);  $^1\text{H}$  NMR ( $\text{CDCl}_3$ ):  $\delta$  3.46 (dd, 1H,  $J$  = 17.34, 6.54,  $\text{CH}_2$ ), 3.81 (s, 3H,  $\text{OCH}_3$ ), 3.99 (dd, 1H,  $J$  = 17.32, 11.96,  $\text{CH}_2$ ), 5.68 (dd, 1H,  $J$  = 11.88, 6.52, CH), 6.77 (s, 1H, aromatic H), 6.90 (d, 2H,  $J$  = 8.72, aromatic H), 7.04 (t, 2H,  $J$  = 8.76, aromatic H), 7.40 (d, 2H,  $J$  = 8.68, aromatic H), 7.53–7.55 (m, 2H, aromatic H), 7.68 (dd, 2H,  $J$  = 8.80, 5.48, aromatic H), 7.86–7.95 (m, 4H, aromatic H), 8.15 (dd, 1H,  $J$  = 8.62, 1.58, aromatic H);  $^{13}\text{C}$  NMR ( $\text{CDCl}_3$ ):  $\delta$  43.37 (pyrazoline  $\text{CH}_2$ ), 55.28 ( $\text{OCH}_3$ ), 64.30 (pyrazoline CH), 102.86, 114.05, 115.14, 115.36, 123.48, 126.38, 126.69, 126.98, 127.51, 127.59, 127.89, 129.96, 128.34, 128.46, 129.18, 131.38, 133.14, 133.88, 133.94, 150.61, 151.70, 159.15, 161.07, 163.52, 164.97; MS  $m/z$ : 480.46 ( $\text{M}^+$ , 16.55 %), 153.25 (100 %). Anal. Calcd. For  $\text{C}_{29}\text{H}_{22}\text{FN}_3\text{OS}$  (479.57): C, 72.63; H, 4.62; N, 8.76. Found: C, 72.89; H, 4.76; N, 8.98.

**4.1.2.15. 4-(1-(4-(4-Fluorophenyl)thiazol-2-yl)-3-(naphthalen-2-yl)-4,5-dihydro-1H-pyrazol-5-yl)-N,N-dimethylaniline (5o).** Yellow solid; yield 76 %; m.p. 268–270 °C; IR (KBr,  $\text{cm}^{-1}$ ): 3043 (CH aromatic), 2947, 2889 (CH aliphatic), 1550, 1485 (C=C);  $^1\text{H}$  NMR (DMSO):  $\delta$  2.84 (s, 6H, N ( $\text{CH}_3$ )<sub>2</sub>), 3.45 (dd, 1H,  $J$  = 17.72, 5.68,  $\text{CH}_2$ ), 4.06 (dd, 1H,  $J$  = 17.66, 11.82,  $\text{CH}_2$ ), 5.63 (dd, 1H,  $J$  = 11.66, 5.74, CH), 6.68 (d, 2H,  $J$  = 8.52, aromatic H), 7.19–7.26 (m, 4H, aromatic H), 7.31 (s, 1H, aromatic H), 7.57–7.59 (m, 2H, aromatic H), 7.81 (dd, 2H,  $J$  = 7.98, 5.90, aromatic H), 7.96–8.01 (m, 3H, aromatic H), 8.06 (d, 1H,  $J$  = 8.56, aromatic H), 8.19 (s, 1H, aromatic H);  $^{13}\text{C}$  NMR (DMSO):  $\delta$  40.52 (N( $\text{CH}_3$ )<sub>2</sub>), 43.22 (pyrazoline  $\text{CH}_2$ ), 64.31 (pyrazoline CH), 104.30, 112.68, 112.85, 115.72, 115.93, 123.48, 127.32, 127.61, 127.94, 128.01, 128.21, 128.81, 128.87, 129.16, 129.38, 131.65, 133.31, 133.87, 149.94, 150.35, 153.30, 164.68; Anal. Calcd. For  $\text{C}_{30}\text{H}_{25}\text{FN}_4\text{S}$  (492.62): C, 73.15; H, 5.12; N, 11.37. Found: C, 73.41; H, 5.39; N, 11.59.

## 4.2. Biological evaluation

All the animal research experiments that involve the performed *in vivo* studies were authorized by the research ethics committee (REC), Faculty of Pharmacy, Cairo University, Egypt, Approval No. PC 3163, at 28/11/2022. Adult male albino mice and Male Wister albino rats were purchased from National Research Centre. All the animal experiments were performed according to National Institutes of Health Guide for the Care and Use of Laboratory Animals (NIH 1985).

### 4.2.1. Analgesic activity evaluation

Adult male albino mice (weight = 20–25 g) were used to study the analgesic activity. Suspension of the tested compounds and the reference standard indomethacin was prepared in 2 % Tween 80. The *p*-benzoquinone-induced writhing method in mice was utilized to evaluate the analgesic activity, and standard laboratory conditions of temperature

and light were used throughout the experimental evaluation, according to previously reported procedures and methods [58–60]. The detailed experimental procedures are shown in [Supplementary material](#).

### 4.2.2. Anti-inflammatory activity

Male Wister albino rats (120–180 g) were resided in the animal house under standard conditions regarding lighting and temperature with free availability of food and water. Compounds, **5a**, **5c**, **5d**, **5e**, **5f**, **5h**, **5m**, and **5o**, in addition to Indomethacin (standard reference) were evaluated compared to untreated control for the anti-inflammatory activity, using the carrageenan-induced rat paw edema model, as described before ([Supplementary material](#)) [49]. Measurement was taken at two different time intervals; 2 h and 3 h and the calculation for this measurement is as follows [59,60]:

$$\% \text{potency} = \frac{\% \text{ edema inhibition for the treated group with the tested compounds}}{\% \text{ edema inhibition for the treated group with indomethacin}}$$

### 4.2.3. Ulcerogenic liability

Adult male albino rats weighing 120–180 g were used for conducting the experimental ulcerogenic liability study, according to reported method [50]. For further details see the [Supplementary material](#). Ulcer index was determined for each compound according to the method of Robert *et al.* [61]. Degree of ulcerogenic effect was calculated in terms of: (a) The incidence of ulcers in each group of animals is divided by ten, expressed as a percentage, (b) The mean number of ulcers per stomach, (c) The visual observation method was used to determine the average severity of ulcers, (d) The total value of the above three mentioned values was used to calculate the ulcer index.

### 4.2.4. Toxicological study

Adult male albino mice (weight range 20–26 g) were used to perform the toxicological study. Mice were classified into 10 groups, five animals in each group. The first group served as a control and received only the dosing vehicle 2 % Tween 80, while the second group received indomethacin the reference standard and the rest of the groups received the tested compounds. This study was performed via multiple increasing intraperitoneal doses up to 10 folds of the used analgesic and anti-inflammatory dosage. The observed mortalities were recorded at each dose level in each group along 24 h, to determine the lowest dosage required to cause mortality in all animals and the highest dosage that did not cause any mortalities.

### 4.2.5. In vitro COX inhibition assay

The inhibitory effects of compounds **5h** and **5m** toward COX-1 and COX-2 were studied using the commercial COX-1 Inhibitor Screening Kit (Fluorometric) Cat. # K548 and COX-2 Inhibitor Screening Kit (Fluorometric) Cat. # K547. The employed technique relies on using fluorescence to detect prostaglandin G<sub>2</sub>, which is an intermediate substance that is produced by COX enzyme. This method is utilized for the screening of inhibitors targeting both COX-1 and COX-2 enzymes. Serial dilutions from the tested compounds, in addition to Celecoxib I and Indomethacin as reference standards, at concentrations of 1, 0.3, 0.1, 0.03, 0.01, 0.003, 0.001 and 0.0003  $\mu\text{M}$  were utilized. The assay was carried out according to the provided instructions in the kit protocol. IC<sub>50</sub> values were calculated using GraphPad Prism 8 analysis software (Graph-Pad, San Diego, CA, USA) from the dose–response curves of eight concentrations for each tested compound [52].

## 4.3. Molecular docking

Molecular modeling simulations of compounds **5h**, **m** were achieved utilizing Molecular Operating Environment (MOE 2019.0101) software package. The generated 3D diagrams were obtained using UCSF Chimera software package [62]. The X-ray crystal structures of COX-1 and COX-2 enzymes (PDB: 1EQG [55] and 3LN1 [56], respectively) were retrieved from RSCB protein data bank [63]. The protein crystal



structures were optimized for modeling by removing chains B; COX-1, and B-H; COX-2 that are not involved in binding interactions. Water molecules further than 4.5 Å from ligand or active site were removed (all water molecules). The crystal structures preparation involved using Protonate 3D protocol. Modeling protocols were validated efficiently, which proved suitability of the prepared COX-1 and COX-2 crystal structures with energy scores of  $-7.48$  and  $-9.92$  kcal/mol, and RMSD values of  $0.8765$  and  $0.0553$  Å, respectively (Supplementary Material, Figures 10S and 11S).

Compounds **5h,m** were prepared for docking simulations using the default MOE setting by energy minimization until an RMSD gradient of  $0.05$  kcal/mol  $-1$  Å $^{-1}$  with MMFF94x forcefield. The lowest energy conformer of each compound was used as an initial conformer for the intended modeling simulation. The docking analysis was achieved by using Triangle Matcher placement method and London dG scoring function. The obtained poses were subjected to force field refinement using GBVI/WSA dG scoring function.

#### 4.4. *In vivo* pharmacokinetic study

As an application of the developed UPLC-MS/MS method, the simultaneous determination of compounds **5d** and **5h** in rat plasma for their *in vivo* pharmacokinetic study was achieved. Ten male Sprague-Dawley rats weighting 250–300 g were purchased from National Research Centre. The animals were housed using standard conditions of temperature and light. All animals had free access to standard laboratory diet. In all tests, adequate precautions were adopted in strict accordance with The Institutional Animal Care and Use Committee ethical standards. The rats were randomly divided into two groups, each group was composed of 5 animals for **5d** and **5h**. Each group was subcutaneously injected with a dose of 10 mg/kg. The compounds were formulated in 5 % tween 80 and normal saline. Blood samples were withdrawn from the retro-orbital plexus following a single administration and transferred into Eppendorf tubes containing 50 µL heparin at the following time intervals: 0, 0.25, 0.5, 1, 2, 4, 6, 8 and 24 h. The collected blood samples were centrifuged at 4000 rpm for 10 min. Then the plasma was separated and stored at  $-20$  °C before analysis. An aliquot of 200 µL of the thawed plasma samples were spiked with 20 µL IS then processed and analyzed. Pharmacokinetic parameters ( $C_{max}$ ,  $T_{max}$ ,  $t_{1/2}$ ,  $AUC_0-t$ ,  $AUC_0-\infty$  and  $Cl$ ) of **5d** and **5h** were calculated using the non-compartmental method, utilizing the WinNonlin software (V 8.3). For the detailed information regarding the method development and validation stages and results see Supplementary Material.

#### CRediT authorship contribution statement

**Eman R. Mohammed:** Writing – review & editing, Writing – original draft, Supervision, Methodology, Data curation, Conceptualization. **Aliaa H. Abd-El-Fatah:** Writing – original draft, Investigation, Funding acquisition, Formal analysis, Data curation. **Abdalla R. Mohamed:** Writing – review & editing, Writing – original draft, Software, Conceptualization. **Marianne A. Mahrouse:** Writing – review & editing, Validation, Supervision, Project administration, Conceptualization. **Mohammad A. Mohammad:** Validation, Supervision, Project administration, Funding acquisition.

#### Declaration of competing interest

The authors declare that they have no known competing financial interests or personal relationships that could have appeared to influence the work reported in this paper.

#### Appendix A. Supplementary data

Supplementary data to this article can be found online at <https://doi.org/10.1016/j.bioorg.2024.107372>.

#### References

- [1] D. Michels da Silva, H. Langer, T. Graf, Inflammatory and molecular pathways in heart failure—ischemia, HFpEF and transthyretin cardiac amyloidosis, *Int. J. Mol. Sci.* 20 (2019) 2322.
- [2] X. Zhang, X. Wu, Q. Hu, J. Wu, G. Wang, Z. Hong, J. Ren, L. for Trauma. Mitochondrial DNA in liver inflammation and oxidative stress, *Life Sci.* 236 (2019) 116464.
- [3] R. Medzhitov, Inflammation 2010 new adventures of an old flame, *Cell* 140 (2010) 771–776.
- [4] N. Singh, D. Baby, J.P. Rajguru, P.B. Patil, S.S. Thakkannavar, V.B. Pujari, Inflammation and cancer, *Ann. Afr. Med.* 18 (2019) 121.
- [5] L. Chen, H. Deng, H. Cui, J. Fang, Z. Zuo, J. Deng, Y. Li, X. Wang, L. Zhao, Inflammatory responses and inflammation-associated diseases in organs, *Oncotarget* 9 (2018) 7204.
- [6] P. Sriutha, B. Sirichanchuen, U. Permsuwan, Hepatotoxicity of nonsteroidal anti-inflammatory drugs: a systematic review of randomized controlled trials, *Int. J. Hepatol.* 2018 (2018).
- [7] K.A. Walker, B.N. Ficek, R. Westbrook, Understanding the role of systemic inflammation in Alzheimer's disease, *ACS Chem. Neurosci.* 10 (2019) 3340–3342.
- [8] T.R. Sampson, J.W. Debelius, T. Thron, S. Janssen, G.G. Shastri, Z.E. Ilhan, C. Challis, C.E. Schretter, S. Rocha, V. Gradinaru, Gut microbiota regulate motor deficits and neuroinflammation in a model of Parkinson's disease, *Cell* 167 (2016), 1469–1480. e1412.
- [9] S. Kim, J. Koh, S.G. Song, J. Yim, M. Kim, B. Keam, Y.T. Kim, J. Kim, D.H. Chung, Y.K. Jeon, High tumor hexokinase-2 expression promotes a pro-tumorigenic immune microenvironment by modulating CD8 $^{+}$ /regulatory T-cell infiltration, *BMC Cancer* 22 (2022) 1120.
- [10] J.-P. Pelletier, J. Martel-Pelletier, F. Rannou, C. Cooper, Efficacy and safety of oral NSAIDs and analgesics in the management of osteoarthritis: Evidence from real-life setting trials and surveys, *Semin Arthritis Rheum.* 45 (2016) S22–S27.
- [11] R. Langenbach, S.G. Morham, H.F. Tian, C.D. Loftin, B.I. Ghanayem, P. C. Chulada, J.F. Mahler, C.A. Lee, E.H. Goulding, K.D. Kluckman, Prostaglandin synthase 1 gene disruption in mice reduces arachidonic acid-induced inflammation and indomethacin-induced gastric ulceration, *Cell* 83 (1995) 483–492.
- [12] S.L. Tilley, T.M. Coffman, B.H. Koller, Mixed messages: modulation of inflammation and immune responses by prostaglandins and thromboxanes, *J. Clin. Invest.* 108 (2001) 15–23.
- [13] D. Mukherjee, Traditional NSAIDs and coxibs: is one better than the other? *Eur. Heart J.* 38 (2017) 1851–1852.
- [14] D. Picot, P.J. Loll, R.M. Garavito, The X-ray crystal structure of the membrane protein prostaglandin H2 synthase-1, *Nature* 367 (1994) 243–249.
- [15] J.R. Kiefer, J.L. Pawlitz, K.T. Moreland, R.A. Stegeman, W.F. Hood, J.K. Gierse, A. M. Stevens, D.C. Goodwin, S.W. Rowlinson, L.J. Marnett, Structural insights into the stereochemistry of the cyclooxygenase reaction, *Nature* 405 (2000) 97–101.
- [16] M. Hawash, N. Jaradat, M. Abualhasan, M.T. Qaoud, Y. Joudeh, Z. Jaber, M. Sawalmeh, A. Zarour, A. Mousa, M. Arar, Molecular docking studies and biological evaluation of isoxazole-carboxamide derivatives as COX inhibitors and antimicrobial agents, *Biotech* 12 (2022) 342.
- [17] A. Alsayari, Y.I. Asiri, A.B. Muhsinah, M. Hassan, Anticancer properties of pyrazole derivatives acting through xanthine oxidase inhibition, *J. Oncol.* 2021 (2021).
- [18] A.A. Bekhit, S.N. Nasralla, S.A. Bekhit, A.-E.-D.-A. Bekhit, Novel dual acting antileishmanial agents derived from pyrazole moiety, *Biointerface Res. Appl. Chem.* 12 (2022) 6225–6233.
- [19] G. Li, Y. Cheng, C. Han, C. Song, N. Huang, Y. Du, Pyrazole-containing pharmaceuticals: target, pharmacological activity, and their SAR studies, *RSC Med. Chem.* 13 (2022) 1300–1321.
- [20] T.D. Penning, J.J. Talley, S.R. Bertenshaw, J.S. Carter, P.W. Collins, S. Docter, M. J. Graneto, L.F. Lee, J.W. Malecha, J.M. Miyashiro, Synthesis and biological evaluation of the 1, 5-diarylpyrazole class of cyclooxygenase-2 inhibitors: identification of 4-[5-(4-methylphenyl)-3-(trifluoromethyl)-1 H-pyrazol-1-yl] benzenesulfonamide (SC-58635, celecoxib), *J. Med. Chem.* 40 (1997) 1347–1365.
- [21] P. Prasit, Z. Wang, C. Brideau, C.-C. Chan, S. Charleson, W. Cromlish, D. Ethier, J. Evans, A. Ford-Hutchinson, J. Gauthier, The discovery of rofecoxib, [MK 966, VIOXX®], 4-(4-methylsulfonylphenyl)-3-phenyl-2 (5H)-furanone], an orally active cyclooxygenase-2 inhibitor, *Bioorganic Med. Chem. Lett.* 9 (1999) 1773–1778.
- [22] M.A. Chowdhury, K.R. Abdellatif, Y. Dong, D. Das, M.R. Suresh, E.E. Knaus, Synthesis of celecoxib analogues possessing a N-difluoromethyl-1, 2-dihydropyrid-2-one 5-lipoxygenase pharmacophore: biological evaluation as dual inhibitors of cyclooxygenases and 5-lipoxygenase with anti-inflammatory activity, *J. Med. Chem.* 52 (2009) 1525–1529.
- [23] E.K. Abdelall, G.M. Kamel, Synthesis of new thiazolo-celecoxib analogues as dual cyclooxygenase-2/15-lipoxygenase inhibitors: Determination of regio-specific different pyrazole cyclization by 2D NMR, *Eur. J. Med. Chem.* 118 (2016) 250–258.
- [24] J.A. Cairns, The coxibs and traditional nonsteroidal anti-inflammatory drugs: a current perspective on cardiovascular risks, *Can. J. Cardiol.* 23 (2007) 125–131.
- [25] R.P. Mason, M.F. Walter, H.P. McNulty, S.F. Lockwood, J. Byun, C.A. Day, R. F. Jacob, Rofecoxib increases susceptibility of human LDL and membrane lipids to oxidative damage: a mechanism of cardiotoxicity, *J. Cardiovasc. Pharmacol.* 47 (2006) S7–S14.
- [26] K.R. Abdellatif, W.A. Fadaly, G.M. Kamel, Y.A. Elshaier, M.A. El-Magd, Design, synthesis, modeling studies and biological evaluation of thiazolidine derivatives containing pyrazole core as potential anti-diabetic PPAR-γ agonists and anti-inflammatory COX-2 selective inhibitors, *Bioorg. Chem.* 82 (2019) 86–99.

- [27] Z. Ju, M. Li, J. Xu, D.C. Howell, Z. Li, F.-E. Chen, Recent development on COX-2 inhibitors as promising anti-inflammatory agents: The past 10 years, *Acta Pharm. Sin. b.* 12 (2022) 2790–2807.
- [28] M. Schattenkirchner, Meloxicam: a selective COX-2 inhibitor non-steroidal anti-inflammatory drug, *Expert Opin Investig Drugs* 6 (1997) 321–334.
- [29] R.N. Sharma, F.P. Xavier, K.K. Vasu, S.C. Chaturvedi, S.S. Pancholi, Synthesis of 4-benzyl-1, 3-thiazole derivatives as potential anti-inflammatory agents: an analogue-based drug design approach, *J. Enzyme Inhib. Med. Chem.* 24 (2009) 890–897.
- [30] X. Ye, W. Zhou, Y. Li, Y. Sun, Y. Zhang, H. Ji, Y. Lai, Darbufelone, a novel anti-inflammatory drug, induces growth inhibition of lung cancer cells both in vitro and in vivo, *Cancer Chemother. Pharmacol.* 66 (2010) 277–285.
- [31] R.D. Kamble, R.J. Meshram, S.V. Hese, R.A. More, S.S. Kamble, R.N. Gacche, B. S. Dawane, Synthesis and in silico investigation of thiazoles bearing pyrazoles derivatives as anti-inflammatory agents, *Comput. Biol. Chem.* 61 (2016) 86–96.
- [32] N.D. Gaikwad, S.V. Patil, V.D. Bobade, Synthesis and antimicrobial activity of novel thiazole substituted pyrazole derivatives, *J. Heterocycl. Chem.* 50 (2013) 519–527.
- [33] S. Mamatha, S. Belagali, M. Bhat, B.K. Joshi, Design, synthesis and characterization of novel Benzothiazolyl pyrazoles as potential antitubercular scaffold, *Chem. Data Collect.* 41 (2022) 100930.
- [34] A.R. Sayed, S.M. Gomha, F.M. Abdelrazek, M.S. Farghaly, S.A. Hassan, P. Metz, Design, efficient synthesis and molecular docking of some novel thiazolyl-pyrazole derivatives as anticancer agents, *BMC Chemistry* 13 (2019) 1–13.
- [35] E. Bansal, V. Srivastava, A.J.E.j.o.m.c. Kumar, Synthesis and anti-inflammatory activity of 1-acetyl-5-substitute daryl-3-( $\beta$ -aminonaphthyl)-2-pyrazolines and  $\beta$ -(substitute daminoethyl) amidonaphthalenes, *Eur. J. Med. Chem.* 36 (2001) 81–92.
- [36] S.N.A. Bukhari, X. Zhang, I. Jantan, H.L. Zhu, M.W. Amjad, V.H. Masand, Synthesis, molecular modeling, and biological evaluation of novel 1, 3-diphenyl-2-propen-1-one based pyrazolines as anti-inflammatory agents, *Chem Biol Drug Des.* 85 (2015) 729–742.
- [37] G.S. Hassan, S.M. Abou-Seri, G. Kamel, M.M. Ali, Celecoxib analogs bearing benzofuran moiety as cyclooxygenase-2 inhibitors: design, synthesis and evaluation as potential anti-inflammatory agents, *Eur. J. Med. Chem.* 76 (2014) 482–493.
- [38] X.-B. Wang, H.-J. Li, Z. Chi, X. Zeng, L.-J. Wang, Y.-F. Cheng, Y.-C. Wu, A novel mitochondrial targeting fluorescent probe for ratiometric imaging SO<sub>2</sub> derivatives in living cells, *J. Photochem. Photobiol. A Chem.* 390 (2020) 112339.
- [39] P. Salehi, M.M. Khodaei, M.A. Zolfigol, A. Keyvan, Solvent-free crossed aldol condensation of ketones with aromatic aldehydes mediated by magnesium hydrogensulfate, *Monatsh. Chem.* 133 (2002) 1291–1295.
- [40] P. Amutha, S. Nagarajan, Synthesis and antimicrobial activities of new 4, 6-diaryl-4, 5-dihydro-3-hydroxy-2H-indazoles, *J. Heterocycl. Chem.* 49 (2012) 428–432.
- [41] K. Krishna Mohan Rao, P. Marutatmaja Rao, Direction of enolization of 1: 3-diketones by mass spectrometry, in: *Proceedings of the Indian Academy of Sciences-Section A*, Springer, 1975, pp. 262–270.
- [42] M.H. Ahmed, M.A. El-Hashash, M.I. Marzouk, A.M. El-Naggar, Synthesis and antitumor activity of some nitrogen heterocycles bearing pyrimidine moiety, *J. Heterocycl. Chem.* 57 (2020) 3412–3427.
- [43] A.O. Abdelhamid, Z.H. Ismail, M.S. El Gendy, M.M. Ghorab, Reactions with hydrazoneyl halides 53: 1 synthesis and antimicrobial activity of triazolino [4, 3-a] pyrimidines and 5-arylazothiazoles, *Phosphorus, Sulfur Relat. Elem.* 182 (2008) 2409–2418.
- [44] D. Kaminsky, B. Bednarczyk-Cwynar, O. Vasylenko, O. Kazakova, B. Zimenkovsky, L. Zaprutko, R. Lesyk, Synthesis of new potential anticancer agents based on 4-thiazolidinone and oleanane scaffolds, *Med. Chem. Res.* 21 (2012) 3568–3580.
- [45] S. Hu, D. Liu, C. Yan, M. Cai, An efficient heterogeneous gold (I)-catalyzed hydration of haloalkynes leading to  $\alpha$ -halomethyl ketones, *Synth. Commun.* 48 (2018) 2983–2991.
- [46] M. Ye, Y. Wen, H. Li, Y. Fu, Q. Wang, Metal-free hydration of aromatic haloalkynes to  $\alpha$ -halomethyl ketones, *Tetrahedron Lett.* 57 (2016) 4983–4986.
- [47] S.A. Laufer, D.R. Hauser, A.J. Liedtke, Regiospecific and highly flexible synthesis of 1, 4, 5-trisubstituted 2-sulfanylimidazoles from structurally diverse ethanone precursors, *Synthesis* 2008 (2008) 253–266.
- [48] R. Okun, S.C. Liddon, L. Lasagna, The effects of aggregation, electric shock, and adrenergic blocking drugs on inhibition of the “writhing syndrome”, *J. Pharmacol. Exp. Ther.* 139 (1963) 107–109.
- [49] C.A. Winter, E.A. Risley, G.W. Nuss, Carrageenin-induced edema in hind paw of the rat as an assay for antiinflammatory drugs, *Proc. Soc. Exp. Biol. Med.* 111 (1962) 544–547.
- [50] M. Meshali, H. El-Sabbagh, A. Foda, Effect of encapsulation of flufenamic acid with acrylic resins on its bioavailability and gastric ulcerogenic activity in rats, *Acta Pharm. Technol.* 29 (1983) 217–219.
- [51] D.J. Finney, *Statistical Method In Biological Assay*, Charles Griffin & Company, 1978.
- [52] P.A. Halim, H.H. Georgey, M.Y. George, A.M. El Kerdawy, M.F. Said, Design and synthesis of novel 4-fluorobenzamide-based derivatives as promising anti-inflammatory and analgesic agents with an enhanced gastric tolerability and COX-inhibitory activity, *Bioorg. Chem.* 115 (2021) 105253.
- [53] M. Hawash, N. Jaradat, R. Sabobeh, M. Abualhasan, M.T. Qaoud, New thiazole carboxamide derivatives as COX inhibitors: design, synthesis, anticancer screening, in silico molecular docking, and ADME profile studies, *ACS Omega* 8 (2023) 29512–29526.
- [54] M. Hawash, N. Jaradat, M. Abualhasan, M.K. Şüküroğlu, M.T. Qaoud, D. C. Kahraman, H. Daraghme, L. Maslamani, M. Sawafta, A. Ratrou, Design, synthesis, molecular docking studies and biological evaluation of thiazole carboxamide derivatives as COX inhibitors, *BMC Chemistry* 17 (2023) 11.
- [55] B.S. Selinsky, K. Gupta, C.T. Sharkey, P.J. Loll, Structural analysis of NSAID binding by prostaglandin H<sub>2</sub> synthase: time-dependent and time-independent inhibitors elicit identical enzyme conformations, *Biochemistry* 40 (2001) 5172–5180.
- [56] J.L. Wang, D. Limburg, M.J. Graneto, J. Springer, J.R.B. Hamper, S. Liao, J. L. Pawlitz, R.G. Kurumbail, T. Maziasz, J.J. Talley, The novel benzopyran class of selective cyclooxygenase-2 inhibitors. Part 2: The second clinical candidate having a shorter and favorable human half-life, *Bioorganic Med. Chem. Lett.* 20 (2010) 7159–7163.
- [57] T.R. Zipp, Z. Izzah, C. Åberg, C.T. Gan, S.J. Bakker, D.J. Touw, J.F. Van Boven, Clinical value of emerging bioanalytical methods for drug measurements: a scoping review of their applicability for medication adherence and therapeutic drug monitoring, *Drugs* (2021) 1–20.
- [58] R.G. Kurumbail, A.M. Stevens, J.K. Gierse, J.J. McDonald, R.A. Stegeman, J.Y. Pak, D. Gildehaus, J.M. Iyashiro, T.D. Penning, K. Seibert, Structural basis for selective inhibition of cyclooxygenase-2 by anti-inflammatory agents, *Nature* 384 (1996) 644–648.
- [59] S.S. Panda, A.S. Girgis, H.H. Honkanadavar, R.F. George, A.M. Srou, Synthesis of new ibuprofen hybrid conjugates as potential anti-inflammatory and analgesic agents, *Future, Med. Chem.* 12 (2020) 1369–1386.
- [60] R.N. Naumov, S.S. Panda, A.S. Girgis, R.F. George, M. Farhat, A.R. Katritzky, Synthesis and QSAR study of novel anti-inflammatory active mesalazine-metronidazole conjugates, *Bioorganic Med. Chem. Lett.* 25 (2015) 2314–2320.
- [61] A. Robert, J.E. Nezamis, J.P. Phillips, Effect of prostaglandin E1 on gastric secretion and ulcer formation in the rat, *Gastroenterology* 55 (1968) 481–487.
- [62] E.F. Pettersen, T.D. Goddard, C.C. Huang, G.S. Couch, D.M. Greenblatt, E.C. Meng, T.E. Ferrin, UCSF Chimera—a visualization system for exploratory research and analysis, *J. Comput. Chem.* 25 (2004) 1605–1612.
- [63] H. Berman, K. Henrick, H. Nakamura, J.L. Markley, The worldwide Protein Data Bank (wwPDB): ensuring a single, uniform archive of PDB data, *Nucleic Acids Res.* 35 (2007) D301–D303.